Ours The Task Eternal

A MULTI-DEVICE MICROWAVE OSCILLATOR USING MICROSTRIP CIRCUITRY

BY

S.T. OGLETREE

CARLETON UNIVERSITY
FACULTY OF ENGINEERING
TECHNICAL REPORT

MARCH 1973

A MULTI-DEVICE MICROWAVE OSCILLATOR
USING MICROSTRIP CIRCUITRY

by

S.T. Ogletree, B.Eng. (Carleton)

This report was prepared for the
Department of Communications
Communications Research Center under
Contract No. OGR2-0073

Carleton University
Ottawa, Ontario

March 1973

ACKNOWLEDGEMENTS

The author wishes to express his gratitude to his thesis supervisor, Dr. V. Makios, for his help during the course of this thesis program. The privilege of using the facilities of the Communications Research Centre, Ottawa, for the experimental work associated with this thesis is gratefully acknowledged. A debt of gratitude is also owed by the author to several members of the staff of the Communications Research Centre, who aided him in various phases of this work. The author is grateful for the suggestions, comments, and constructive criticism offered by Dr. W.J. Chudobiak, and for the technical assistance rendered by Mr. R. Mann and Mr. M. Walker.

During the course of this thesis program, the author was aided by Dr. D.R. Conn, who gave generously of his time and experience. For this, the author offers his sincere thanks.

The financial support provided by the Department of Communications (OGRO-222 and OGR2-0073) is gratefully acknowledged.

Without the patience and encouragement of his wife Anne, the author would never have been able to undertake this thesis. The author wishes to express his deepest gratitude to his wife and three children, Susan, Carol and Ruth, for the patient way in which they accepted the various deprivations involved.

ABSTRACT

A method of combining microwave solid-state devices in a microstrip oscillator circuit to obtain high output power, is presented in this thesis. Several problems associated with the design and operation of multi-device oscillator circuits are discussed. Possible solutions to these problems are illustrated by a series of two-device circuit designs. The result is a circuit which effectively combines the output power from two devices.

The circuits described in this thesis use commercially available IMPATT diodes in microstrip transmission line circuit configurations. The design frequency of operation is 10 GHz, with performance results given for the frequency band of 9.5 to 10.5 GHz. The performance results are based upon a CW mode of operation.

Single-diode microstrip oscillator circuits are also studied, to provide support for the multi-device studies. From this study, microstrip circuit design guidelines are derived. Furthermore, references are established which are then used in the evaluation of the two-diode circuit experiments.

TABLE OF CONTENTS

TABLE OF CONTENTS (Cont'd)

LIST OF FIGURES

LIST OF FIGURES (Cont'd)

LIST OF FIGURES (Cont'd)

LIST OF SYMBOLS

AM	Amplitude Modulation
B_s	Open-ended transmission line stub susceptance
β	Imaginary component of the propagation constant of a wave travelling along a transmission line
C	Capacitance
C_d	Diode Capacitance
ϵ_r	Relative dielectric constant of the microstrip transmission line substrate material
dB	Decibels
dBm	Power ratio in decibels referred to 1 milliwatt
dBW	Power ratio in decibels referred to 1 watt
DC	Direct Current
Δ	Incremental
f	Frequency
f_o	Frequency below which dispersion is negligible
FM	Frequency Modulation
G_d	Diode Conductance
g_l	Parasitic load conductance of microstrip circuitry
GHz	Gigahertz
h	Thickness of the substrate material of microstrip transmission line
IMPATT	IMPact Avalanche Transit Time
j	$(-1)^{\frac{1}{2}}$

LIST OF SYMBOLS (Cont'd)

l	Length in metres
l'	Length in wavelengths
L	Inductance
λ	Wavelength of an electromagnetic wave
λ_m	Wavelength of the propagating wave on a microstrip transmission line
mA	milliampere
MHz	Megahertz
mil	10^{-3} inches
mW	milliwatt
N_1/N_2	Primary to Secondary turns ratio
ω	Angular frequency in radians
ω_o	Resonant angular frequency in radians
π	3.14159
P_o	Output power
P_{in}	Input power
PRF	Pulse Repetition Frequency
Q	Quality factor
Q_{ext}	External quality factor
R	Resistance
R_d	Diode Resistance (real part of the diode impedance)
R_L	Real part of the load impedance

LIST OF SYMBOLS (Cont'd)

R_o	Real part of the transmission line characteristic impedance
R_T	Real part of a transformed impedance
RF	Radio Frequency
TRAPATT	TRApped Plasma Avalanche Transit Time
w	Width of the strip conductor of a microstrip transmission line
X-band	Common designation of the frequency spectrum from 8.0 to 12.4 GHz
X_d	Reactive or imaginary component of the diode impedance
Y	Admittance
Y_d	Diode admittance
Y_o	Characteristic admittance of a transmission line
Z	Impedance
Z_d	Diode impedance
Z_i	Input impedance
Z_L	Load impedance
Z_o	Characteristic impedance of a transmission line
Z_{out}	Output impedance
Z_P	Impedance looking into a parallel equivalent circuit
Z_{PP}	Impedance looking into two parallel equivalent circuits in parallel

LIST OF SYMBOLS (Cont'd)

Z_s	Impedance looking into a series equivalent circuit
Z_{sp}	Impedance looking into two series equivalent circuits in parallel
Z_T	Transformed impedance

CHAPTER I

INTRODUCTION

1.1 Introduction

There is an ever increasing demand for reliable, microwave sources in the $\pm$ 10 dBW power range. The applications range from communications and navigational aids through to laboratory and research programs. Solid-state, two-terminal devices, partially fill the power requirement, as indicated by figure 1.1. Furthermore, solid-state devices offer the desired reliability.

To meet the power requirements, research is being conducted in two main areas. The first area concerns the improvement of the device. The second area involves the development of circuits which sum the output power from several devices. This thesis describes research conducted in the latter area. In particular, this thesis deals with IMPATT diodes combined in microstrip circuit configurations operating at X-band frequencies.

1.2 Literature Survey of Active, Two-Terminal, Solid-State Device Combination Techniques

In September 1967, Swan et al[2] reported work on mounting several individual silicon avalanche devices in parallel, on a single header. The result was that the individual devices performed as a single device having a large area. Because of the physical separation of the devices, the thermal distribution problems inherent in large area devices were, to some extent, avoided. On the basis of their work, Swan et al concluded that:

(i) the output power was directly proportional to the total device area (i.e. the number of individual devices in the composite structure),

(ii) the efficiency remained unchanged relative to the number of devices used, since it is proportional to the power density in the device rather than the active area.

These results are consistent with those stemming from single device studies.

The work reported in June 1971, by Cowley and Patterson[3] is an extension of that reported by Swan et al[2]. Whereas Swan et al fabricated several devices and then bonded them to a common header, Cowley and Patterson describe a technique whereby the devices are fabricated as a single entity. The results obtained from this structure are comparable to those reported by Swan et al but due to the greater ease of fabrication, a substantial economic benefit is realized.

Similar research has been reported by Mitsui[4], using Gunn devices in a composite structure. Using resistivity, active area, and bias current as variables, Mitsui found experimentally a set of parameters which yielded the highest output power and efficiency when employed in a two-device composite structure. He also experimented with three and four device composite structures but was unable to obtain the high output power that was expected from these structures. This was due to problems encountered in matching the composite structure impedance to a standard load. An inherent disadvantage in composite structures is their low output impedance. As the number of devices is increased in the structure, the combined impedance is lowered and hence the problem of matching to a standard RF load impedance (i.e. 50 ohms in a coaxial circuit) is increased.

Another technique for combining devices, and one which avoids the impedance problem mentioned above, is the series connection of devices. In October 1967, Carroll[5] reported on experiments performed on two and four Gunn diodes operating in series in a coaxial circuit. In all cases it was found that the output power from the combination was higher than the sum of the output power of the diodes, when measured individually. Carroll offers two possible explanations for these results:

i) the parasitic loading by the circuit was less for the combined diodes than for the single diode experiments,

ii) the output from the diodes in series may have included spurious components which were not present during the single diode measurements. The author was unable to ascertain the spectral purity of the output by means of spectrum analysis, since he was operating from a pulsed bias source with a low PRF.

Magalhaes and Schlosser[6], performed similar experimental work using three IMPATT diodes in series. Unlike Carroll[5], the authors observed that the output power from the combined devices was equal to the sum of the power of the diodes when measured individually. Furthermore, their experimental work showed that the output power was independent of the spacing between the diodes within the coaxial cavity.

A disadvantage of the series operation of devices as described in the above papers[5,6] was that the bias source was common to all the devices. A short circuit failure in one device could induce failure in the remaining devices due to excessive voltage across the devices. An open circuit failure in one device would render the entire circuit inoperative. This method of combining devices would then appear undesirable for commercial applications.

However, Blair et al[7] describe an application in which four Gunn devices were mounted in series for use in a phased array radar system. Endurance testing performed on one of ten modules produced for this system proved successful, thus generating optimism for the series connected method of combination. The reliability of the Gunn devices coupled with the thermal design of the diode mounts made this approach feasible.

In May 1968, Boronski[8] reported on experimental work in which several Gunn diodes were combined in parallel in a waveguide structure. The combined output power was slightly less than that predicted by adding the power from the same diodes operating individually. A similar experiment was reported by Schlosser and Stillwell[9], using a stripline circuit which yielded comparable results. To avoid the multi-mode problem[9,11,20] associated with multiple-device oscillator circuits, they used a locking source which was isolated from the combined devices.

Another method of paralleling devices in a waveguide configuration was given by Ivanek and Reddi[10]. In this paper, it was reported that the combined power exceeded the sum of the power of the individual devices by three percent. The authors noted that the frequency of operation of the parallel combination differed substantially from the frequency at which the devices operated individually. They offered, as an explanation for this result, that the efficiency of the devices was a function of the frequency of operation.

In December 1969, Rucker[11] successfully paralleled five IMPATT diodes in a coaxial module. A method of suppressing instabilities arising from the operation of two or more devices in a common circuit was presented, along with two observations which make the parallel method of combining attractive. First, he found that he was able to operate the combined devices at a significantly higher input power level, (and hence obtain a correspondingly higher output power), than that predicted by multiplying the maximum permitted input power per device by five. Secondly, Rucker found a substantial decrease in the AM noise power generated by the combined diodes relative to a prediction based upon five times the noise power generated by a single device. This resulted in an improved carrier-to-noise ratio which indicated that while the carrier power was additive, the noise power from each diode was averaged. Kurokawa[12], followed up the work by Rucker with an analysis of the circuit. This analysis confirmed mathematically the experimentally observed stability of the circuit.

Kostishack[13] reported the successful combination of three Fairchild type FD 300 diodes operating in the TRAPATT mode[14]. This parallel combination yielded extremely high peak power and efficiency at UHF frequencies.

The concept of combining sources has been in existence for several decades. Generally, the objective has been to phase-lock a high power source to a lower power, but more stable one. In this way, the low power source stabilizes the high output power source. This concept has been extended to avalance diode circuits operating at microwave frequencies. Socci and Harrison[15] reported the combination of two independent avalanche diode circuits. The combined output power was higher than the sum of the power from the individual circuits. Socci and Harrison attribute this to the extra loss presented to the circuit by the short which was used to replace one of the diodes during the single diode circuit evaluation. It was also shown that high power level injection locking of the avalanche device could be achieved by coupling the circuit to a stable laboratory source. The frequency stability of the avalanche diode circuit was enhanced in this manner.

Fukui[16] presented a general case circuit in which any number of devices may be effectively combined. He established criteria which had to be met in the circuit for the addition of power to occur. The concept of phase-locking the individual active devices with each other within the circuit was employed. Subsequent to Fukui's work, Luzzatto[17] described theoretically another device combining circuit. However, his circuit relied on coherent and equi-power sources to be combined. Hence, this circuit was impractical since the design failed to relate to the real problems encountered in device combination. Mizushina[18] dealt with the problem of device combining through the use of 3 dB directional couplers. Unfortunately, his experimental work was conducted in the low megahertz region and hence there is some doubt as to the applicability of the method at microwave frequencies.

An interesting method of combining two devices is suggested by Kuno et al[19]. The method employs the push-pull concept. The RF circuit is in fact a series configuration although the devices are biased in parallel. From a power generation point of view, this method is attractive since the theoretical output power is twice the sum of the power of the individual devices. The authors' experimental work resulted in the achievement of about seventy-five percent of the theoretical output power.

A significant development in multi-device microwave sources was reported by Kurokawa and Magalhaes[20]. The authors achieved more than 10 watts of power at 9.1 GHz, using twelve IMPATT diodes coupled into a single waveguide cavity. Each diode was mounted in the end of a coaxial line, the opposite end of which was terminated by a tapered absorber. The coaxial lines were coupled to the side wall of a single waveguide cavity at half-wavelength spacings. The use of a common, high Q cavity eliminated the multi-mode problem. A follow-up paper by Kurokawa[21] supported the work with a detailed mathematical analysis of the method. He also showed that the mean square values of the amplitude and frequency fluctuations of the output signal are inversely proportional to the number of devices in the circuit. Thus, as the number of devices increases, both the AM and FM noise components are decreased. This further substantiates the observations made by Rucker[11].

1.3 Thesis Rationale, Approach and Objectives

The literature survey of the previous section reveals that the bulk of the research work in the area of microwave device combination has centred upon waveguide and coaxial circuit concepts. Another form of microwave circuitry, using microstrip transmission lines is becoming increasingly popular. Microstrip offers several distinct advantages to both the researcher and the manufacturer, over the more conventional microwave circuits.

The increased usage of printed circuits in the electronics industry over the past two decades has resulted in a highly refined fabrication technique. Microstrip, which is in fact an extension of the printed circuit concept, takes advantage of this development. To the researcher, the short time between design and fabrication of a circuit is attractive. The manufacturer experiences an economic benefit from microstrip circuitry in that the expensive machining operations associated with waveguide and coaxial circuitry are eliminated.

In conjunction with the expanding microwave integrated circuit research program at Carleton University, this thesis deals with microstrip circuitry as a medium by which avalanche devices are combined to provide high output power microwave sources.

An experimental approach to the problem of combining several discrete devices in a microstrip circuit has been adopted, rather than a theoretical study. The literature survey tends to justify such an approach. In papers where a theoretical argument is presented[12,21], it is based upon a previous report of experimental observations[11,20].

The objectives of this thesis may be summarized as follows:

(i) To study single-diode microstrip circuits, as a basis for multi-device circuits. The single-device circuit performance can then be used as a reference for evaluating multi-device circuits.

(ii) To develop a two-device microstrip circuit which may be used as a basis for power combination studies.

1.4 Thesis Organization

A general introduction to the work is given in chapter 2 by way of an investigation of the components used in realizing the circuits to be studied. Design guidelines are established which define the minimum and maximum values for the characteristic impedance of the microstrip transmission lines. An experimentally determined value is found for the parasitic load conductance which the microstrip circuitry presents to the active device. From the investigation of the characteristics of the active device used, a design frequency of operation, as well as a bias level for the device is established. Chapter 2 then carries on to a study of single-device oscillator circuits. Methods of providing the necessary conditions for oscillation to occur are discussed. The purpose for the study of single-device oscillators is to provide a base from which to commence the study of multi-device circuits and hence combination techniques, and also to establish a reference by which multi-device circuit performance may be evaluated.

Two-device circuit designs and their subsequent evaluations are then presented in chapter 3. The various approaches to multi-device circuit design suggested in the literature survey are considered, and where possible, are adapted to microstrip circuitry. Several design proposals are presented, each of which attempts to provide a solution to a previously encountered problem associated with multi-device circuit operation. Eventually, a circuit evolves which acts as an effective device combiner.

Chapter 4 summarizes the work and draws several conclusions from the work presented in chapters 2 and 3. Suggestions for further work in the area of multi-device, microwave sources, are also presented.

CHAPTER 2

SINGLE-DEVICE CIRCUIT STUDIES

2.1 Introduction

To provide a basis for the study of multi-device circuits, a preliminary study of single-device circuits was undertaken. Prior to considering circuit designs, however, several practical aspects of fabricating microstrip transmission lines are discussed. From these considerations, guidelines are established which are then employed in the design work which follows. Other design specifications such as the frequency of operation and bias current level are chosen, based upon an examination of the active device to be used in the circuits. Several design approaches are investigated in this chapter. The outcome is a single-device oscillator design which is then used as the basis for multi-device circuit studies.

A set of reference measurements were performed on a set of four diodes in single-device circuits for use in evaluating the performance of multi-device circuits using the same diodes.

2.2 Microstrip Circuit Considerations

The microstrip circuitry used for the work described in this thesis was fabricated from a commercially available, copper clad teflon material*. The dielectric thickness (h) was 10 mils, with a 1 mil thickness of copper on either side. The relative dielectric constant (ϵ_r) of the substrate material was 2.35. A complete listing of the specifications of this material as given by the manufacturer is included in appendix A. The value of such material for research work lies in the ease with which microstrip circuits may be fabricated from it. Normal printed circuit etching techniques are applicable. Also, various modifications to a fabricated circuit are possible in the laboratory by simply cutting away sections of the copper with a knife.

There were several aspects of microstrip transmission lines which were investigated as an integral part of the design work described in this thesis. It was found that losses within the microstrip circuit could not be neglected and still achieve a good match of the diode impedance to a load. Dispersion in microstrip transmission lines was considered, as well as the edge fringing field effect of open-ended lines. Consideration was also given to the methods

---

*RT/duroid, type 5870.

available for fabricating microstrip circuitry. From these investigations, a set of design guidelines were developed which were then applied to the circuit designs which are described in this thesis.

There is an apparent disagreement among researchers as to the calculation of loss in microstrip transmission lines. The work on microstrip transmission line loss, first published by Assadourian and Rimai[22], is disputed by Purcel et al[24]. It is however recognized that three distinct components of microstrip loss exist;

(i) conductor loss (including loss in the groundplane),
(ii) dielectric loss,
(iii) radiation loss.

The method of determining the radiation loss component seems to account for the uncertainty surrounding the calculation and measurement of microstrip losses. Lewin[25], shows that radiation from microstrip is due to discontinuities. Pucel et al[24] describe the effort taken to fabricate "discontinuity-free" microstrip lines in order to make accurate dielectric and conductor loss measurements.

In view of the complexity of microstrip loss characterization, and the stated objectives of this thesis, a precise determination of the losses associated with the microstrip circuitry was not attempted. Instead, an experimental approach was adopted wherein all the loss components were lumped into one value. A loss conductance, g_L , was assumed as a parasitic load presented by the microstrip circuit to the diode. The value of g_L was then determined from the results of a set of experiments. A single device oscillator was developed, (see section 2.5) and several versions tested, each of which assumed a different value of g_L from zero to two millimhos in half millimho steps. The output power as a function of frequency was measured. The dependency of output power upon external tuning* was also observed. The results of this set of experiments are given in figures 2.1 to 2.5. The criteria used to evaluate the data and hence choose a value for g_L was;

(i) output power,

(ii) flatness of the output power across the frequency band of 9.5 to 10.5 GHz,

(iii) the dependence of output power upon external tuning.

Figure 2.3 yields the best results with respect to the above criteria in that for this data the maximum power and flatness was achieved while a minimum dependency upon

*E-H tuner - see figure C1.

external tuning was observed. This indicated that for a circuit in which a one millimho loss element was assumed, the best match between the diode and the load was achieved. The value of one millimho for g_L was retained in subsequent work and applied to each device used in multi-device circuits.

Another parameter of microstrip transmission lines considered was dispersion. The frequency below which dispersion is negligible is given by Jain[26] as;

$$f_o = \frac{6.0}{(\epsilon_r - 1)^{1/4}} \left[\frac{Z_o}{h}\right]^{1/2} \qquad (2.1)$$

where; ϵ_r = relative dielectric constant of the substrate material,

Z_o = characteristic impedance of the propogating wave on the microstrip transmission line,

h = thickness of the substrate material in mils,

f_o = frequency in GHz.

Throughout the work presented in this thesis, a design frequency of 10 GHz has been assumed. From equation (2.1) it is seen that line impedances of $Z_o \geq 32.5$ ohms may be used without encountering dispersive effects. This consideration is the basis on which a lower limit on the characteristic impedance of $Z = 35$ ohms was applied to the microstrip transmission lines used in this thesis.

The upper limit upon the characteristic impedance was based upon fabrication considerations. Standard printed circuit board etching techniques dictate a minimum line width of about 5 mils for consistent results. To fabricate line widths narrower than 5 mils, the more elaborate procedures followed in semiconductor fabrication must be employed. However, the physical size of the total microstrip circuit is greater than that which may be conveniently handled in a semiconductor fabrication laboratory. Referring to Wheeler's curves[28], (see figure 2.6c), we find that a line width of 5 mils corresponds to a characteristic impedance of 122 ohms. Thus, values of characteristic impedance in the range of $32.5 \leq Z_o \leq 122$ ohms were used in all microstrip circuit designs reported in this thesis, except for circuit configuration B1 (see section 3.3.1).

Open-ended tuning stubs were used in the circuit designs, however no edge fringing field correction was applied. Jain et al[27], have shown that this effect is negligible for the material used in this thesis.

Calculation of the required geometrical configurations for the microstrip circuits were based upon Wheeler's curves[28]. These curves are given in figure 2.6.

2.3 Description of the Active Device

The active devices used in the circuits reported in this thesis were Hewlett-Packard, model 5082-0435 IMPATT diodes. This device is designed to operate in the frequency band from 8 to 12 GHz, with a typical output power of 100 milliwatts (in a circuit with $Q_{ext} = 40$). The choice of 10 GHz as the design frequency for the circuits reported in this thesis is thus justified as this frequency lies in the centre of the band of operation of the device. A complete description and list of the manufacturer's specifications for this device is included in appendix A. The packaged diode terminal admittance at 10 GHz was taken to be -3+j80 millimhos. This value was determined experimetally[29].

A bias current of 40 milliamps per diode was used throughout the experimental work reported in this thesis. This value was chosen because it permitted stable operation of the device while avoiding excessive thermal build-up within the circuit. It was found that this bias level was sufficient to provide a safe condition under which to conduct extended experiments with both single and multi-device circuits. Appendix B considers the method of biasing the device and describes the circuit used to provide the constant current source.

2.4 General Circuit Design Philosophy

Basic oscillator theory states that oscillation will occur if, at some frequency, the load impedance is the negative of the impedance of the active device. There are two basic approaches which may be followed in order to satisfy this condition. The first approach is to assume the series equivalent circuit of the packaged device (represented by the terminal impedance). The required load is then the series configuration illustrated by figure 2.7a. The second approach assumes the parallel equivalent circuit of the packaged diode (represented by the terminal admittance), requiring the load configuration shown in figure 2.7b.

2.4.1 Series Equivalent Configuration

In a microstrip circuit, the series reactive element is realized by a fixed section of line. This is undesirable from an experimental point of view since no adjustment to the circuit may be made. The real part of the diode impedance, which is very low (typically -0.5 ohms) must be matched to a fixed load impedance which is 100 times greater (i.e. 50 ohms). This may be accomplished by the use of a quarter-wave transformer, but in microstrip, this necessitates the use of a wide line section having the following two disadvantages. The first is that the effects of dispersion are no longer negligible and hence the calculations of the line geometry are more complex. Secondly, the width of the line becomes comparable to a wavelength at the frequency of operation. This then requires a two-dimensional analysis of the line section rather than the one-dimensional analysis normally considered in microstrip theory. The following numerical calculation will illustrate this point.

Consider a packaged diode whose terminal impedance is given by -0.46-j12.3 ohms. For oscillation, a load impedance of 0.46+j12.3 ohms must be presented to the diode. The approach followed here will be to transform the diode impedance by means of a line section, to the point where the imaginary part of the impedance is zero. The diode then is reactively tuned, leaving the real part, which then may be matched to a real load impedance by using a quarter-wave transformer.

Assuming the microstrip line to be a low loss transmission line, the transformed impedance, Z_T, of an impedance Z_d, by a line of length L and characteristic impedance Z_o, is given by[30];

$$Z_T = \frac{Z_o Z_d \cos\beta l - j Z_o^2 \sin\beta l}{Z_o \cos\beta l - j Z_d \sin\beta l} \qquad \text{(2.2)}$$

where; $\beta = \dfrac{2\pi}{\lambda_m}$

$\lambda_m =$ wavelength in the microstrip line under consideration.

Assume that the characteristic impedance of the microstrip line has a real part only, denoted by R_o. Rationalizing equation (2.2) and separating Z_T into real and imaginary components;

$$Re\left[Z_T\right] = \frac{R_o^2 R_d}{R_o^2 + R_o X_d \sin 2\beta l + X_d^2 \sin^2\beta l} \qquad \text{(2.3)}$$

$$Im\left[Z_T\right] = \frac{R_o\left[(R_d^2 + X_d^2 - R_o^2)\sin 2\beta l + 2R_o X_d \cos 2\beta l\right]}{2\left(R_o^2 + R_o X_d \sin 2\beta l + X_d^2 \sin^2\beta l\right)} \qquad \text{(2.4)}$$

where; $R_d = Re\left[Z_d\right]$

$X_d = Im\left[Z_d\right]$

We require that the transformation be such that the imaginary component becomes zero.

i.e. $R_o\ (R_d^2 + X_d^2 - R_o^2)\sin 2\beta l + 2R_o X_d \cos 2\beta l = 0$ ___ (2.5)

Dividing equation (2.5) by $\cos 2\beta l$ we have;

$$R_o\ (R_d^2 + X_d^2 - R_o^2)\tan 2\beta l + 2R_o X_d = 0 \qquad \text{(2.6)}$$

or;

$$\tan 2\beta l = \frac{2 R_o X_d}{R_o^2 - R_d^2 - X_d^2} \qquad \text{(2.7)}$$

Hence the required length of the transmission line (in metres) is given by

$$L = \frac{1}{2\beta} \tan^{-1}\left[\frac{2R_o X_d}{R_o^2 - R_d^2 - X_d^2}\right] \qquad (2.8)$$

or in terms of wavelengths;

$$L' = \frac{1}{4\pi} \tan^{-1}\left[\frac{2R_o X_d}{R_o^2 - R_d^2 - X_d^2}\right] \qquad (2.8a)$$

By substituting equation (2.8) into (2.3), an expression for the transformed impedance $R_T = Re\left[Z_T\right]$ is given.

For a diode impedance Z = -0.46-j12.3 ohms and a transmission line characteristic impedance of Z_o = 50 ohms, using equation (2.8a) we get L' = 0.03935 . Calculating the value for L from equation (2.8) and using this value in equation (2.3) gives R_T = 0.411 ohms. The values for both L' and R_T may be verified on a Smith Chart.

It is now required to match R_T to a real load impedance R_L. This may be done by using a quarter-wave transformer section, the characteristic impedance of which is given by[31];

$$Z_{o1} = \left(|R_T|\, R_L\right)^{1/2} \qquad (2.9)$$

For the example under consideration, Z_{o1} = 4.54 ohms.

Referring to figure 2.6a, for $\epsilon_r = 2.35$ and $h = 10$ mils, we obtain a $^W/_h$ ratio of 53. Therefore w is 530 mils. Referring to figure 2.6b, for $^W/_h = 53$, we get a ratio of 1.5. Taking λ_o to be 1181 mils at 10 GHz , λ_m equals 787.3 mils. Hence the width of the transformer section is 0.673 λ_m.

It can thus be concluded that this design is unsatisfactory because the effect of dispersion must now be considered (i.e. Z_{01} = 4.54 ohms, $\angle$ 32.5 ohms), and also because the width of the section is a significant fraction of a wavelength.

2.4.2 Parallel Equivalent Configuration

Use of the parallel equivalent circuit approach allows the use of open-ended stubs at the diode to parallel tune the diode susceptance component. This configuration takes advantage of the adjustment feature of the microstrip material. The stubs may be shortened, thereby permitting upward frequency tuning of the circuit.

The real part of the diode admittance which remains after addition of the stubs, may be matched to the load admittance by means of a quarter-wave transformer. Since the real part of the diode admittance is lower than the load admittance, the transformer section will consist of a narrow line, thus eliminating the problem discussed in section 2.4.1. However, in practice it was found that the opposite extreme was the case, i.e. the line width was too narrow to be fabricated using normal printed circuit etching techniques.

To illustrate this, consider the following example. Assume that a diode admittance of $-3+j80$ millimhos is to be matched to a load of 20 millimhos and that a parasitic load, due to the microstrip circuit, of 1 millimho is also presented to the diode. The characteristic impedance of the quarter-wave transformer necessary to transform 20 millimhos to 2 millimhos is 158.1 ohms (from equation 2.9). From figure 2.6c, for $\epsilon_r = 2.35$ and $h = 10$ mils, we obtain a W/h ratio of 0.25, and hence $W = 2.5$ mils. As noted in section 2.2, a line width less than 5 mils was impractical to fabricate and hence this circuit was abandoned.

2.4.3 The Cascaded Quarter-Wave Transformer Concept

The reason for rejecting the circuits discussed in sections 2.4.1 and 2.4.2 was due to the quarter-wave matching transformer. It has been found however, that the use of several sections in series will permit matching, while still maintaining the condition that $32.5 \leq Z_o \leq 122$ ohms for the characteristic impedance of the sections. Furthermore, it was found that three stages were sufficient to meet the requirements of the parallel equivalent circuit configuration and four stages for the series equivalent configuration. The use of this concept is demonstrated in the circuits discussed in the following sections.

2.5 Single-Device Circuits

2.5.1 Circuit Configuration AI (figure 2.8)

The parallel equivalent circuit approach was initially adopted for single-device circuit studies for two reasons. First, this method allows an upward frequency adjustment by shortening the diode resonating stubs. This feature has been discussed in sections 2.2 and 2.4.2. Secondly, it was hypothesized that this approach would be tolerant to parasitic series impedances induced by fabrication defects, such as etching pits, in the microstrip circuitry. Since the real part of the resonated diode impedance is large in this configuration, a small residual series resistance would result in a small amount of mismatching. Any residual reactive components could be corrected by adjustment of the diode stubs.

Two open-ended stubs in parallel were used to resonate the diode. This was done as an experimental convenience. Since the diode susceptance is capacitive at 10 GHz, an inductive element is required to resonate it. Considering an open-ended transmission line as the inductive element, its susceptance is given by;

$$B_s = j\, Y_o \tan \beta L \qquad (2.10)$$

where; Y_o = characteristic admittance of the transmission line,

L = length of the transmission line.

$\tan \beta L$ is a slowly varying function of L for small values of B_s. Hence, by dividing the inductive susceptance between two open-ended transmission lines, a more easily controlled variation of the total inductive susceptance as a function of length was possible. This in turn permitted a finer adjustment of the frequency of operation of the circuit.

The design impedance parameters calculated for circuit configuration AI are given by figure 2.8a. They are based on a frequency of operation of 10 GHz, and the requirement to match to a 50 ohm load. As an example of the method used to design the microstrip circuitry reported in this thesis, the steps taken to arrive at these design values are as follows:

a) Stub length

It is required that each of the stubs present an inductive susceptance of 40 millimhos parallel to the diode admittance of 20 millimhos, then equation (2.10) gives $l = 0.324\lambda$. An extra length of 0.1λ was then added for purposes of adjustment.

b) First Quarter-Wave Transformer Section

The resonated diode admittance is -3 millimhos. The loss component determined in section 2.2 (g_l = 1 millimho) was then added, which gave a net conductance of -2 millimhos (or in terms of impedance (Z_1), -500 ohms). The characteristic impedance of the first quarter-wave transformer section was arbitrarily chosen to be 50 ohms. Applying equation (2.9), the output impedance is calculated as;

$$Z_{out_1} = \frac{(50)^2}{-500}$$

$$= -5 \text{ ohms}, \; (-Z_L)$$

c) Second Quarter-Wave Transformer Section

To apply equation (2.9) to the second quarter-wave transformer section, either the characteristic impedance or the output impedance must be arbitrarily chosen. Since a limit has been established for the minimum value of the line characteristic impedance, the value in this case was taken to be 35 ohms (Z_{o2}).

Hence;

$$Z_{out_2} = \frac{(35)^2}{-5}$$

$$= -245 \text{ ohms } (-Z_3)$$

d) Third Quarter-Wave Transformer Section

The purpose of the third quarter-wave section is to match -245 ohms to 50 ohms. Applying equation (2.9) again, given;

$$Z_o = (\,|-245|\, \times 50)^{\frac{1}{2}}$$

$$= 110.7 \text{ ohms } (Z_{o3})$$ - the characteristic impedance of the third quarter-wave transformer section.

The dimensions given by figure 2.8b were obtained by using Wheeler's curves[28] for the various impedance values given above. It should be noted that the length of the first transformer section was increased by 60 mils to accommodate the diode package flange (indicated by the dashed circle).

A typical IMPATT diode (denoted D4) was used to test this circuit. The diode was biased at 40 milliamps from a constant current source. The output power and efficiency as a function of frequency was measured over the frequency range of 9.5 to 10.5 GHz. The dependency of the output power on external tuning was also monitored. The results of these measurements are presented graphically in figure 2.9.

Circuit configuration A1 performed well as a single-diode source, but when used as the basis for a double device circuit, the performance was unsatisfactory (see sections 3.3.3 and 3.3.4). The argument given in section 2.5.2, based upon the experimental observations given in section 3.3.4, prompted the design of the next circuit configuration.

2.5.2 Circuit Configuration A2 (figure 2.11)

Consider a single section quarter-wave transformer. The input impedance in terms of the characteristic impedance and output impedance is given by:

$$Z_i = \frac{Z_o^2}{Z_L} \qquad (2.11)$$

where Z_i = input impedance,

Z_o = characteristic impedance,

Z_L = output impedance.

Differentiating Z_i with respect to Z_L :

$$\frac{dZ_i}{dZ_L} = -\frac{Z_o^2}{Z_L^2}$$

$$= -\frac{Z_i}{Z_L} \qquad (2.12)$$

In terms of increments of impedance:

$$\Delta Z_i = -\frac{Z_i}{Z_L}\Delta Z_L \qquad (2.12a)$$

It can thus be seen from equation (2.12a) that perturbations in the output impedance are amplified at the input when the ratio of input to output impedance is greater than 1. A double degradation occurs in the oscillator where the output or load impedance perturbation contains both resistive and reactive components. The real part of the perturbation causes a mismatch while the reactive component detunes the circuit. It is thought that this was the cause of the unsatisfactory performance resulting from the attempt to use circuit configuration A1 as part of a multi-device configuration. Although equation (2.12a) was developed from the consideration of a single stage quarter-wave transformer, the same relationship can be shown to hold for three cascaded quarter-wave transformers.

It would then appear from the above reasoning that a configuration which yields the lowest negative resistance to be matched to the load, should be used, particularly in the case where load impedance perturbations are to be expected. However, as noted by Mitsui[4], the lower the device impedance, the greater the difficulty in matching that impedance to the load.

The series equivalent configuration discussed in section 2.4.1 offers a circuit in which the negative resistance is low. A disadvantage to the configuration is that the circuit is not frequency tunable. However, a single device circuit was developed which made use of the low negative resistance of the series equivalent configuration and the tunability of the parallel equivalent configuration. The Smith Chart shown in figure 2.10 gives a graphical interpretation of the design philosophy of circuit configuration A2. Point A represents the admittance which the external circuit must present to the diode in order to meet the requirements for oscillation and impedance matching. (The parasitic load conductance of 1 millimho has also been added at this point). Two stubs are then added to the diode which place an inductive susceptance of 30 millimhos each, in parallel with the diode admittance. This then places the combined admittance at point B on the Smith Chart. An eight-wavelength series section of microstrip transmission line transforms the impedance at point B to point C. The diode is now resonated and the real impedance which remains is higher than that of the series equivalent configuration but lower than the load impedance. The use of stubs to partially resonate the diode permits frequency tuning of the circuit. The curves D-E, F-G, and H-I represent the first, second and third stages of the cascaded quarter-wave transformer sections respectively.

The calculated admittance and impedance values used in the design of circuit configuration A2 are shown on a physical layout of the circuit in figure 2.11. The circuit was tested, using diode D2 biased with a constant current of 40 milliamps. The output power as a function of frequency over a band from 9.5 to 10.5 GHz was measured along with the DC to RF conversion efficiency. The output power dependency upon external tuning was also observed. Figure 2.12 gives the results of this test.

Circuit configuration A2 operated well as a single-device circuit. Its performance in a multi-device configuration is reported in chapter 3.

2.6 Single-Diode Circuit Reference Measurements

To evaluate multi-device circuits, a reference was required. This reference was acquired by using four IMPATT diodes, denoted D1 to D4, in circuit configuration A2. The output power and efficiency as a function of frequency over the band of 9.5 to 10.5 GHz was measured. The dependency of output power upon external tuning was also observed in each case. The same four diodes were then used in the study of multi-device circuits. The results of the measurements for diode D1 are given in figure 2.3. The results for diode D2 are given in figure 2.12. Figures 2.13 and 2.14 give the results of measurements using diodes D3 and D4, respectively. These results are then used as a reference for evaluating the performance of the multi-device circuits presented in the following chapter.

CHAPTER 3

THE DEVELOPMENT OF A TWO-DEVICE OSCILLATOR CIRCUIT

3.1 Introduction

Two-device circuits were used as the basis for the study of combining active devices in an oscillator. This approach maintained the experimental complexity at a minimum while at the same time exposing the problems associated with multi-device oscillator circuits. The groundwork laid in chapter 2 was used to its fullest extent in the work presented in chapter 3. As previously noted, some of the work of chapter 2 was initiated as a result of two-device circuit considerations. Some of the experimental results of chapter 2 were used as a reference in the evaluation of the results of this chapter.

The bulk of the work in this chapter consists of a report on a series of two-device circuit designs, and the experimental test results obtained from each one. Each design attempted to deal with a specific problem encountered in the previous design. Most of the problems were anticipated as a result of the literature survey presented in chapter 1. From this process, a circuit evolved which performed as an effective, active device power combiner.

3.2 Basic Multi-Device Circuit Design Considerations

There are three general approaches to the design of multi-device oscillator circuits using packaged devices in a microstrip transmission line structure. These approaches may be summarized as follows;

i) Close grouping the devices within the circuit so that they may be considered as a single device.

ii) Couple each device individually to a common cavity.

iii) Incorporate each device in a circuit and then combine the output from each circuit.

The objective in closely grouping the devices is to simulate a composite structure[2,3,4]. This approach was considered at an early stage of this thesis program and subsequently abandonned. It was found to be impossible to conduct sufficient heat away from the devices to permit extended CW operation of the circuit, using normal heat-sinking techniques. A possible solution to this problem would have been to operate the diodes from a pulse bias source. However, this was considered to be an impractical method of studying multi-device circuits, since there would be an ambiguity as to whether steady-state conditions had been reached during the pulse period. An attempt to physically separate the devices within the circuit leads to either the second or third approach listed above.

Several authors[5,6,7,8,11,13,20] have described circuits in which the common cavity concept was employed. This approach was used in the first multi-device circuit studied in this thesis program. A detailed report of the experimental observations is presented in a later section. The results were not encouraging and the common cavity concept was abandonned in favour of the circuit combination approach.

The work presented in chapter 2 was, to a large extent, initiated by the requirement to obtain a satisfactory single-device circuit which could then be used as the basis for circuit combination work. It was this approach which gave the most encouraging results, as will be shown later in this chapter.

A problem associated with the combination of several devices in an oscillator circuit is that of maintaining the correct phase relationship between the active devices. To illustrate, consider the case where several devices are coupled to a common cavity. The solid arrows shown in figure 3.1 indicate the condition in which the RF currents through all the devices are in phase. There are however, several undesirable modes of oscillation possible[20]. The dashed arrows in figure 3.1 indicate one of the possible undesirable modes in which the RF currents through two of the diodes are out of phase, relative to the remaining diodes. In the case of N diodes symmetrically coupled to a cavity, there are at least N-1 such undesirable modes of oscillation, each of which have essentially the same probability of occurrence. Small variations in loading, biasing, or temperature can cause jumping from mode to mode thereby resulting in frequency and output power instability. This is the well-known multimoding problem associated with multiple-device oscillators.

The multi-mode problem is not confined solely to the common cavity method of achieving multiple-device oscillators. An experiment in which several independent oscillators, each tuned to the same frequency was performed by Schlosser and Stillwell[9]. Their method of eliminating multi-mode operation was to isolate (by means of a circulator), one oscillator from the rest. The isolated oscillator was then free of disturbances from the remaining oscillators while at the same time, providing a signal to which they phase-locked.

Another method of preventing multi-mode operation in multiple-circuit oscillators is to close-couple the independent sources to one another. Each source is then phase-locked to every other source in the circuit. Fukui[16] devised such a circuit in which mutual synchronization of the individual oscillators was achieved. He noted that the frequency stability of the circuit was approximately equal to the most stable oscillator. The conclusions arrived at by Boronski[8] and, Ivanek and Reddi[10] are interesting with respect to phase-locking. In both cases, it was found that a half-wave length spacing between diodes operating in waveguide structures gave the best results. This substantiates Fukui's conclusion that an integral number of half-wavelength spacings between sources was required for maximum frequency stability.

The method of biasing the devices is another important consideration in the design of multi-device circuits. The devices may be individually biased or biased from a common source. If common biasing is used, then the diodes must be selected on the basis of similar static characteristics. Individual biasing permits the use of un-matched devices. Another problem is presented by using IMPATT diodes biased in parallel from a common supply. An open circuit failure in one of the devices may induce an overdrive condition on the remaining devices since IMPATTS are operated from a constant current source. In microstrip transmission line configurations, there are two possible methods of achieving the necessary DC isolation of the individually biased devices. One method involves the use of coupled lines and the other is to use blocking capacitors. The latter method was chosen for the multi-device designs presented in this thesis. This choice was made because little is known about coupled microstrip transmission lines whereas the use of a DC blocking capacitor is a standard technique. Another requirement of the bias circuit is that it should appear as a high impedance to the RF circuits. This is necessary to minimize RF power loss through parasitic loading and reactive de-tuning.

The problem of heat-sinking increases as the number of devices in a multi-device circuit is increased. This problem can be reduced to a great extent, without using sophisticated heat-sinking techniques, by designing the maximum possible physical separation between devices into the configuration. It will be noted that in the double device designs presented in this chapter, device separation has been employed as an aid to heat sinking.

3.3 Two-Device Circuit Configurations

A number of two-device circuits were designed and tested, the results of which are presented in this section. The order in which these designs are presented represents the chronological order in which they were studied. An analysis of the results obtained for a configuration, in general, led to the modification in the design of the succeeding one.

3.3.1 <u>Circuit Configuration BI</u> (figure 3.2)

The common cavity approach was used in the design of circuit configuration BI (see figure 3.2). Two diodes were coupled to a common section of microstrip transmission line. The section of transmission line transformed the parallel impedance, to an impedance for which the imaginary part was zero. This impedance was then transformed by three cascaded quarter-wave transformer sections to match a 50 ohm load. Single, open-ended stubs were added at each diode and at the junction point of the diodes as an experimental convenience in fine tuning the circuit.

The diodes were coupled to the common point by means of a wavelength section of microstrip transmission line. The purpose of this was to permit physical separation of the diodes for heat removal, and also to facilitate the inclusion of DC blocking capacitors. The blocking capacitors were inserted three quarter-wavelengths away from each diode. At this point the diode impedance is transformed from a low to a high value. Any series components introduced by the addition of the capacitor would thus have a minimal effect upon the circuit.

Each diode was biased from a separate source designed to appear as an open circuit at the frequency of operation (10 GHz). The bias circuit consisted of a rectangular section of microstrip transmission line, a half-wavelength long by a quarter-wavelength wide, to which a constant current source was applied. The midpoints of the long sides of the section then appeared as an RF short. One of these points was coupled to the diode package by a quarter-wavelength of 100 ohm characteristic impedance line. The diode thus looked into an open circuited bias line at 10 GHz.

Figure 3.2 shows the layout of circuit configuration B1, along with the design impedance values. These impedance values were calculated on the assumption that each diode has an impedance of -0.46-j12.3 ohms. The impedance at the junction point is then the two diode impedances in parallel, or -0.23-j6.3 ohms ($-Z_2$). The length of 50 ohm characteristic impedance (Z_{01}) microstrip transmission line required to resonate this impedance is found from equation (2.8a) as 0.0198 . The output impedance is calculated from equation (2.3) as -0.22 ohms ($-Z_3$). Three cascaded quarter-wave transformer sections were then used to match to a 50 ohm load impedance. The input/output impedance values, as well as the characteristic impedances of the transformer sections were calculated using equation (2.9) and are shown in figure 3.2. It will be noted that a characteristic impedance of 20 ohms for two of the quarter-wave transformer sections has been used, and that this value is lower than the minimum value established in chapter 2. This is due to the fact that this circuit was designed and tested prior to the establishment of the limits of the characteristic impedance values.

Circuit configuration B1 was tested using diodes D2 and D3, each biased at 40 milliamps of current. It was found that the circuit would operate at two independent frequencies, each frequency variable from 9.2 to 9.9 GHz. This variation in frequency was controlled by adjusting the length of the diode stubs. By carefully adjusting the diode stub lengths, the circuit could be made to operate at a single frequency. However, there was no evidence of phase-locking between the two diodes, even when the frequencies were adjusted to within a few megahertz of one another. The junction stub was found to influence the output power of the circuit, with little effect upon the frequency of operation. The maximum power obtained from configuration B1 was 12 milliwatts at 9.7 GHz. External tuning of the circuit was required to achieve this output power.

The difficulty in matching the low impedance of two diodes in parallel to a load, as well as to each other, was to a great extent responsible for the failure of this configuration to perform as an effective power combiner. This conclusion corresponds to that of Mitsui[4]. Using Gunn devices, - which generally have a higher negative resistance than IMPATT diodes, - Mitsui was unable to effectively combine more than three devices in a composite structure. He concluded that the problem was due to the low impedance resulting from the parallel combination of devices.

3.3.2 <u>Circuit Configuration B2</u> (figure 3.3)

Several features of the parallel equivalent circuit (see section 2.4.2) provided the basis for the design of configuration B2 (see figure 3.3). Each diode was resonated by two open-ended stubs whichalso provided a wider frequency tuning capability than that available in configuration B1. It was anticipated that the high resonated diode impedance would make matching less difficult. A loss component of one millimho for the microstrip circuitry surrounding each diode, (see section 2.2) was incorporated into this design.

The diodes were each connected, in parallel to a common point by a 50 ohm characteristic impedance, wavelength section of microstrip transmission line. A separate bias circuit, similar to that used in configuration B1, was used in each diode. The bias circuit was coupled to the diode at a point a quarter-wavelength away from the diode, on the 50 ohm line. At this point, the diode impedance had been transformed to a low value, thereby reducing any effect that the bias circuit might have had on the RF circuit. A half-wavelength away from each diode on the 50 ohm line, (a high impedance point), the DC blocking capacitors were inserted. The parallel combination of the diode impedances was then matched to a 50 ohm load by three cascaded quarter-wave transformers. The design limits established in chapter 2, on the value of characteristic impedance were observed in the design of circuit configuration B2. Figure 3.3 shows the layout of the microstrip circuit used in configuration B2, along with the relevant design impedance values.

The results of the experimental work performed on circuit configuration B2 are given in figure 3.4 in the form of a graph of output power as a function of frequency over the band of 9.5 to 10.5 GHz. External tuning of the circuit was required to obtain the graph shown in figure 3.4. At several discrete frequencies, the circuit operated without the aid of external tuning. These occurrences are noted as well in figure 3.4. The diodes used in the test of this circuit were D2 and D3, biased to 40 milliamps of current each.

It was found that the frequency of operation of this circuit could be varied by adjusting the stubs associated with either diode. This indicated that the diodes were phase-locked and hence closely coupled to each other. A test was performed to determine the minimum frequency separation required for the circuit to operate at two different frequencies simultaneously. It was found that a minimum separation of 550 MHz was required. This was achieved by adjusting the stubs associated with one of the diodes only.

The output power realized from circuit configuration B2 was slightly less than the power which could be obtained from either diode operating in a single-diode configuration (see figures 2.12 and 2.13). The fact that external tuning was required for oscillation (in most cases), indicated that both matching and tuning problems existed within the circuit. It was hypothesized that the tight coupling between the two diodes might be partially responsible for the poor performance of this configuration. Impedance perturbations due to a change in operating conditions in one of the diodes, would be reflected into the other diode. Thus a design was sought which would provide some decoupling and hence isolation between the two diodes.

3.3.3 Circuit Configuration B3 (figure 3.5)

There are a number of methods available of coupling oscillator circuits together, which may be adapted to microstrip configurations. A method using 3 dB directional couplers is suggested by Mizushina[18]. Such a coupler using microstrip transmission lines has been designed by Reed and Wheeler[32]. Fukui[16] proposed a similar method of coupling, using a rat-race ring. Luzzatto[17] expanded the concept of the rat-race ring to incorporate more than two oscillators into a single circuit. Each of these methods are easily realized in microstrip circuitry.

A more exotic method of coupling, involves the use of circulators. The adaptation of ferrimagnetic devices to microstrip circuits is presently an area of active research[33]. As such, it was not seriously considered as a method of achieving the objectives of this thesis program.

The approach adopted in the design of circuit configuration B3 (see figure 3.5), was somewhat simpler than those listed above. It consisted of inserting quarter-wave transformer sections between the diode and the junction point. This permitted each diode to be individually matched to some fixed impedance. The design proposal was then to take two such circuits in parallel and match the resulting impedance to a load. A distinct advantage to this design method was that each diode and its associated circuit was a complete oscillator and hence the design could be tested prior to its incorporation into a multi-device circuit. It was anticipated that this would be of considerable aid in the isolation of any problems experienced when it formed part of a multi-device circuit. The details of the design of the single-diode sections of configuration B3 are discussed in section 2.5.1 (Circuit Configuration A1).

Circuit configuration B3 was thus formed, as shown in figure 3.5, by joining two configuration A1 circuits via 50 ohm, quarter wavelength sections of microstrip transmission line. The circuits, combined in parallel, had an output impedance of -25 ohms ($-Z_6$) which was then matched to 50 ohms by a quarter-wave transformer with a characteristic impedance of 35 ohms (Z_{o2}). There were two reasons for designing the single-diode parts of the circuit to match to 50 ohms. Since they were designed so that they could be operated individually as single diode circuits, it was necessary to design them to operate into a standard load - which is generally 50 ohms. Secondly, it permitted them to be connected by arbitrary lengths of 50 ohm characteristic impedance transmission line. This was considered desirable, since the DC blocking capacitors were to be inserted into this line and the width of the 50 ohm microstrip transmission line was compatible with the physical size of the capacitors used. It was thought that this would result in a minimal discontinuity due to the capacitors.

The bias circuits and DC blocking capacitors were added to the circuit as shown in figure 3.5. The bias circuit was modified in this configuration. This modification was introduced to further ensure that the bias circuit effects upon the RF circuit were minimal, although there was no positive evidence that the previous design had degraded the circuit performance. The layout, showing the design philosophy of the bias circuit, is described by figure 3.6.

Circuit configuration B3 was tested using diodes D2 and D3 biased at 40 milliamps of current each. It was found to be impossible to obtain stable, single-frequency operation of the circuit. Two simultaneous frequencies of operation were observed to be the preferred mode of operation, but triple-frequency operation could also be achieved under some tuning and operating conditions. In some instances, it was observed that the difference between the two frequencies was less than 10 MHz. Variation of the bias current through the diodes failed to produce stable single-frequency operation.

An output power of 150 milliwatts was measured during double-frequency operation when the separation of the two frequencies was greater than 50 MHz, and both frequencies were within 200 MHz of 10 GHz. The power was measured, using a broadband thermistor. The power was found to decrease as the frequencies approached a single value. No measurements of output power were made during triple-frequency operation. This mode of operation was too unstable to permit accurate measurement of the output power. However, it was observed that the power decreased when the circuit jumped into this mode.

Since it was known that the individual diode circuits used in this configuration would give stable operation at a single frequency, attention was focused upon the method of combining the circuits, in an effort to find an explanation for the observed behaviour of the two-diode circuit. It had been assumed up to this point, in the design of the circuits, that the diode was completely resonated and that any combination involved real impedance components only. This of course is true only at the frequency of operation. An examination of the situation in a frequency band, centred around the design frequency of operation is justified since it is virtually impossible to tune two independent oscillators to operate at <u>exactly</u> the same frequency. The combination of two such oscillators relies upon the interaction between them (phase-locking), for single frequency operation.

Consider the equivalent circuit of an oscillator as seen by the load, over a narrow band of frequencies centred about the frequency of operation. There are two possible basic equivalent circuits, as shown schematically in figure 3.7. Now consider the effect of combining two oscillators in parallel, as proposed by circuit configuration B3. If the combination is symmetrical, then there are again two possibilities, as indicated schematically in figure 3.8. The resistive components of the circuits shown in figures 3.7 and 3.8 are disposed of, in the following discussion. This simplifies the mathematics involved without invalidating the conclusion.

For the series equivalent circuit shown in figure 3.7a:

$$Z_s(\omega) = j\left(\omega L_1 - \frac{1}{\omega C_1}\right) \quad \text{for } R_1 = 0 \qquad (3.1)$$

The parallel combination of two series equivalent circuits (figure 3.8a) gives:

$$Z_{sp}(\omega) = Z_{s1}(\omega) \,/\!/\, Z_{s2}(\omega)$$

$$= j\left[\frac{\omega^4 L_1 C_1 L_2 C_2 - \omega^2 (C_1 L_1 + C_2 L_2) + 1}{\omega^3 C_1 C_2 (L_1 + L_2) - \omega (C_1 + C_2)}\right]$$

$$\text{for } R_1 = R_2 = 0 \qquad (3.2)$$

The function $Z_{sp}(\omega)$ is represented by figure 3.9 for the condition, $L_1C_1 \neq L_2C_2$. That is, the resonant frequencies of the two circuits are different.

Similarly, for the parallel equivalent circuit shown in figure 3.7b:

$$Z_p(\omega) = j\left(\frac{\omega L_1}{1-\omega^2 L_1 C_1}\right) \qquad \text{for } R_1 = \infty \qquad \text{\_\_\_\_\_\_\_\_} \quad (3.3)$$

The parallel combination of two parallel equivalent circuits (figure 3.8b) gives:

$$Z_{pp}(\omega) = Z_{p1}(\omega) // Z_{p2}(\omega)$$

$$= j\left[\frac{\omega L_1 L_2}{L_1 + L_2 - \omega^2 L_1 L_2 (C_1 + C_2)}\right] \qquad \text{for } R_1 = R_2 = \infty \qquad (3.4)$$

The function $Z_{pp}(\omega)$ is represented by figure 3.10 for the condition, $L_1C_1 \neq L_2C_2$.

Figure 3.9 shows that there can be three distinct points of resonance, confined to a narrow band of frequencies, associated with the parallel combination of two series equivalent circuits. This is not the case for the parallel combination of two parallel equivalent circuits, as illustrated by figure 3.10. Here, there is only one point of resonance. It would thus appear from the results of the tests performed on circuit configuration B3, that this circuit is a combination of two series equivalent circuits. A cursory examination of configuration B3 however, does not support this hypothesis. The diode and open-ended stubs form a parallel equivalent circuit. The effect of the three quarter-wave transformer sections is to transform this to a series equivalent circuit*. The quarter-wave section which connects the output of the last quarter-wave transformer to the junction point, transforms the series equivalent circuit back to a parallel equivalent circuit. Hence, it would appear that circuit configuration B3 is a parallel combination of two parallel equivalent circuits. There is therefore, an apparent disagreement between the analysis of the circuit and its experimental behaviour.

It was stated that the circuit analysis was based upon a cursory examination of the circuit. A closer inspection of circuit configuration B3, reveals that the first quarter-wave section after the diode may act possibly as a tapped, resonant transmission line section[34] as well as a quarter-wave transformer. A resonant transmission line section is generally a shorted quarter-wave section and behaves as a

---

*The impendance inversion (paralled/series transformation) effect of a quarter-wave section of transmission line, can be shown by examination of equation (2.2). Let $l = \lambda_m/4$;

then, $Z_T = Z_o^2/Z_d = Z_o^2 Y_d$

For $Z_o = R_o$ (i.e. a real characteristic impedance), the expression $R_o^2 Y_d$ can be modelled by a conductance in parallel with a susceptance, whereas Z_T is modelled as a resistance in series with a reactance.

parallel resonant circuit. In this case, the section is shunted by 5 ohms, rather than a short circuit. This however, gives a reflection coefficient of -0.9 (a short circuit has a reflection coefficient of -1.0). Modelling the first quarter-wave section as a resonant transmission line section then, yields a series equivalent circuit at the junction point of the two single-diode circuits and hence corresponds to the experimental observations. To test this hypothesis, it is only necessary to design and test a circuit in which the quarter-wave section between the last transformer section is either removed or else increased to an even multiple of quarter-wavelengths.

3.3.4 Circuit Configuration B4 (figure 3.5)

The modification of configuration B3 suggested in the previous section was incorporated into configuration B4 (see figure 3.5). The length of the microstrip transmission line joining the output transformer of the single-diode circuits to the junction point was increased from a quarter, to a half wavelength. In all other respects, circuit configuration B4 was identical to B3, as shown in figure 3.5. A test was performed on configuration B4 using diodes D2 and D3, each biased with 40 milliamps of current.

The multi-frequency operation observed in the test of configuration B3 did not occur in this test. In fact it was found that the single-diode circuits had to be deliberately tuned at least 150 MHz apart to obtain double-frequency operation. The results of the test are given in figure 3.11, in the form of a graph of output power and efficiency as a function of frequency. The dependency of the output power on external tuning is also noted in figure 3.11.

Circuit configuration B4 did not yield the output power and efficiency that was expected. Based upon the results of configuration A1 (see figure 2.9), it was anticipated that an output power of 200 milliwatts at 10 GHz could be achieved. It was also anticipated that if the circuit was properly matched, that the dependence upon external tuning would be minimal. The results did however, confirm the hypothesis presented in section 3.3.3 that the first transformer stage acted as a resonant transmission line as well as a quarter-wave transformer.

Based upon the conclusion that mismatch conditions existed in circuit configuration B4, a re-examination of the single-diode sections of the circuit was undertaken. The resulting re-design of the single-diode circuit is discussed in section 2.5.2. The re-designed, single-diode circuit

(circuit configuration A2) was then incorporated into a two-diode configuration as described in the next section.

3.3.5 Circuit Configuration B5 (figure 3.12)

Two configuration A2 circuits were connected in parallel, as shown in figure 3.12, to form configuration B5. It was determined that these circuits should be connected together by half wavelength sections of line as was done in configuration B4. The input quarter-wave transformer section was assumed to act as a resonant transmission line section as well as a quarter-wave transformer. The tap and feed points of the resonant line are reversed with respect to those of configuration B4, but this does not alter its behaviour. The result is that configuration B5 can be modelled as a parallel combination of two parallel equivalent circuits. The bias circuits were connected to the lowest impedance points in the configuration, as indicated in figure 3.12. This was done to further ensure that the bias circuits did not affect the RF circuits.

Testing of circuit configuration B5 was performed using diodes D2 and D3, each biased with 40 milliamps of current. The graph shown in figure 3.13 gives the test results in the form of a plot of output power and efficiency as a function of frequency. The output power dependency upon external tuning is also shown in figure 3.13. To determine the phase-locking bandwidth of the two devices in configuration B5, a test was performed in which one of the single-diode sections of the circuit was tuned to a higher frequency than the other. At the commencement of this test, the circuit operated at 9.82 GHz. The stubs associated with one of the diodes were then progressively shortened until dual-frequency operation was observed. At this point, the two frequencies of operation were 9.79 GHz and 9.93 GHz, thus giving a separation of 140 MHz.

The results of the tests on circuit configuration B5 were considered to be sufficient evidence that an effective combination of two active devices in an oscillator circuit had been achieved. A comparison of the results of configuration B5, with the same diodes operating in single-device configurations is presented in the following section. From this, a measure of the success in combining two avalanche diodes in an oscillator circuit, is obtained.

3.4 Evaluation of the Results of Circuit Configuration B5

The purpose of combining active devices in a single oscillator circuit is to obtain high output power. The ultimate goal is to obtain an output power which is equal to the sum of the output power of the devices when each one is operated in a single-device circuit. Thus, a method of measuring the effectiveness of an oscillator circuit containing more than one active device is available. References were established in chapter two, in which the output power from four diodes, operating in representative, single-device configurations, was measured over the frequency band of 9.5 GHz to 10.5 GHz. Two of these diodes, (D2 and D3) were used in the tests performed on circuit configuration B5. In both the single-diode, and two-diode circuit tests, each diode was biased with 40 milliamps of current, thus permitting a direct comparison of the results.

The output power from diode D2 (figure 2.12), when added to the output power for diode D3 (figure 2.13), gave a value for the output power to be expected from a two-diode circuit containing those diodes. The comparison was then made for circuit configuration B5 by expressing the expected output power divided by the output power from configuration B5 as a ratio in decibels (i.e. $10 \operatorname{Log}_{10} \frac{Po(D2+D3)}{Po(B5)}$). This comparison is presented graphically in figure 3.14 over the frequency band of 9.5 GHz to 10.5 GHz. The comparison was made on the basis of data obtained with, and without the use of external tuning.

Over the band of frequencies considered in figure 3.14, the greatest loss experienced by the combined-diode circuit relative to single-diode operation was 0.77dB for the case where no external tuning was used, and 0.88dB for the case where external tuning was applied. The greatest loss in both cases occurred around the design frequency of operation (10 GHz). This was probably due, to a large extent, to the bandpass properties of the quarter-wave transformers used in the single-diode sections of the circuit. At 10 GHz, the maximum power could be coupled from one of the single-diode sections of the circuit into the other. This would of course, tend to enhance the phase-locking bandwidth of the circuit at frequencies around 10 GHz. No experiments were performed on the circuit to support this hypothesis. As indicated in figure 3.14, there were areas in the frequency band at which higher output power levels than expected, were achieved from configuration B5. These occurrences were however, considered to be insignificant since the application of experimental error to these results could easily suppress the apparent gains.

Circuit configuration B5 thus provides experimental evidence that at least two avalanche-devices may be effectively power combined in a microstrip oscillator circuit. The losses involved are low enough to make this configuration attractive as a power combination circuit.

CHAPTER 4

CONCLUSIONS AND RECOMMENDATIONS

4.1 Summation and Conclusions

A method of effectively combining two avalanche-diodes in a microstrip circuit configuration, to perform as a microwave source, has been presented. Several problems associated with multiple-device circuit design and operation have been defined and dealt with through the presentation of a series of two-diode circuit designs. The major problems encountered, may be summarized as follows:

(i) multi-moding,

(ii) multi-resonance,

(iii) impedance perturbations causing mismatch.

The multi-mode problem was anticipated in advance of the work on two-diode circuits. This problem, as well as its solution, is well documented in the literature[9,11,20]. Phase-locking of the active devices within the circuit prevents multi-moding. To phase-lock the devices, a certain degree of coupling must exist between them. However, in coupling the devices together, each device then loads the remaining devices, thus resulting in a loss of output power. Hence the degree of coupling must be controlled so as to provide the required phase-locking of the devices, without causing excessive loading. This consideration has been an underlying theme in the design and analysis of circuit configurations B2 through to B5.

The inadvertent design of narrowband multiple-resonance into a circuit may cause multi-frequency operation as well as multi-moding. This problem was illustrated in the design of circuit configuration B3. The consideration of multi-resonance in circuits using IMPATT or Gunn devices is more critical than for circuits employing transistors. In the case of a transistor, the frequency range over which it appears as a negative resistance is narrow, being determined by its feedback circuit. However, IMPATT and Gunn devices show a negative resistance over a wide frequency range, often in excess of an octave. Hence, undesirable resonances must be either eliminated or else moved well away from the required frequency of operation. The discussion presented in section 3.3.3 shows one method of eliminating undesired resonances.

The combination of active devices in a circuit in which each device loads the remaining devices, presents a matching problem. Changes in the operating conditions of one of the devices may change its terminal impedance. This in turn causes a change in the loading upon the other devices in the circuit and hence mismatching, with a resultant loss of output power. The analysis of this problem presented in section 2.5.2, leads to a method of minimizing the effect of device impedance perturbations upon the remainder of the circuit.

Circuit configuration B5 represents a solution to the multiple-device oscillator circuit problems discussed above. Although configuration B5 was a two-device circuit, its design concept should be valid for circuits containing more than two devices.

4.2 Recommendations for Further Work

It is believed by the author that the work presented in chapter 3 may be extended to incorporate more than two devices in an oscillator circuit. This could be accomplished by considering the circuit presented in section 3.3.5 (circuit configuration B5) as a single source, and combining it with a similar source in the same manner as the two single-diode sources were combined to form configuration B5. Unfortunately, time limitations prevented this from being accomplished for this thesis. By the combination of both single and two-diode circuits in this manner, it appears possible that any number of devices may be effectively combined.

The only precaution that can be foreseen at this time is that the circuits must be connected by integral multiple lengths of half wavelength sections of transmission line in order to avoid the multi-resonance problem discussed in section 3.3.3.

Kurokawa[12,21] has shown analytically that both the AM and FM noise components of a multi-device oscillator are inversely proportional to the number of devices used in the circuit. This has been experimentally confirmed for multi-device oscillators in coaxial[11] and waveguide[21] circuit configurations. It would thus be appropriate to study the noise characteristics of the multi-device microstrip configuration presented in this thesis.

An interesting observation regarding multi-device oscillator circuits was reported by Rucker[11]. He found that it was possible to operate the devices in a multi-device oscillator at significantly higher input power levels than would be possible in single-device circuits. An experimental re-confirmation, and analysis of this phenomenon would certainly enhance the multiple-device circuit concept for obtaining high output power. The multi-device microstrip circuit configuration presented in this thesis offers a good circuit on which to base such a study. The fact that the multi-device circuit may be broken up into single-device circuits would be advantageous to this study.

The possibility of obtaining a combined output power which is greater than the sum of the outputs from the individual devices should also be studied. Once again, the flexibility of the microstrip circuit presented in this thesis would be of advantage for such a study. Welch and Ishii[35] reported a successful experiment in this area, using two klystrons. Their explanation for their results, was that while both klystrons performed as power sources, they also acted as reflection amplifiers for the signal from each other.

Although IMPATT diodes were used in the work presented in this thesis, it is thought that the concepts employed in the microstrip circuit designs could be applied as well to other solid-state microwave devices such as Gunn, TRAPATT and BARITT diodes, and microwave transistors. Such an extension of this work would not only enhance the multiple-device oscillator concept, but would also contribute to the more general field of Microwave Integrated Circuits.

APPENDIX A

MANUFACTURERS' SPECIFICATIONS FOR THE MICROSTRIP TRANSMISSION LINE MATERIAL AND IMPATT DIODE

As a means of offering a complete description of the components used in the circuits described in this thesis, the manufacturers' specification publications for the microstrip transmission line material and the IMPATT diode are included in this appendix.

Data Sheet • RT/duroids

ROGERS CORPORATION
ROGERS, CONNECTICUT 06263

RT/duroid 5870 - Reinforced Polytetrafluoroethylene

RT/duroid 5870 is a polytetrafluoroethylene laminate reinforced with randomly oriented microglass fibers and designed for exacting electronic and microwave circuit applications. When copper clad, it meets MIL-P-13949 Type GP and also can soon be specified to the new MIL-P-13949 Type GR microwave material specification.

RT/duroid 5870 features excellent X-Band electrical properties. It has the traditional RT/duroid stability in severe environments allowing for ease of fabrication and stability in use. It can be etched hot, soldered, punched, and edge and through-hole plated.

Property	ASTM Method	Test Values*
Reinforcement		Glass Microfiber
Specific Gravity	D792-50	2.15
Tensile Strength, Longitudinal, psi	D638-52T	7500
Tensile Strength, Transverse, psi		5500
Compressibility, 5000 psi, %	D1170-58T	6
Recovery, %		85
Durometer, D Scale		72
Compressive Strength, psi	D695-54	10,000
Stiffness, Longitudinal, lb./sq.in.	D747-50	250,000
Stiffness, Transverse, lb./sq.in.		210,000
Impact Strength, FT.-lb./in.	D256-47T	
Longitudinal, Edgewise		1.4
Longitudinal, Facewise		2.2
Transverse, Edgewise		1.3
Transverse, Facewise		2.4
Flexural Strength, Longitudinal, psi	D790-49T	15,000
Flexural Strength, Transverse, psi		10,000
Coeff. of Friction - against polished steel		
Dynamic, 4000 psi, 2 fpm		0.025
Static, 4000 psi		0.028
Water Absorption, 24 hours- 70°F, %		
1/32" thickness		.3 max.
1/16" through 1/8" thickness		.2 max.
Specific Heat BTU/lb. -°F		0.23
Thermal Expansion Coefficient x 10^{-5}		
Longitudinal Direction, 0-100°F		1.6
Transverse Direction, 0-100°F		4.0
Thickness Direction, 0-100°F		10.0
Longitudinal Direction, 100°-350°F		1.0
Transverse Direction, 100°- 350°F		2.0
Thickness Direction, 100°- 350°F		10.1
Thermal Conductivity, $\frac{\text{BTU - in.}}{\text{hr. - Sq. Ft. -°F}}$		1.8

(over)

Property	ASTM Method	Test Values*
Heat Distortion Temperature, °F	D648-45T	
66 psi		500+
264 psi		500+
Deformation under load, %	D621-51	
122°F, 1200 psi		0.2
2000 psi		0.6
300°F, 1200 psi		1.0
2000 psi		2.0
Dielectric Strength, Short Time, volts/mil.	D149-55T	300
Dielectric Constant, 1 MHz	D1531-58T	2.35
Dissipation Factor, 1 MHz	D1531-58T	0.0005
Dielectric Constant, 10 GHz	MIL-P-13949	2.35
Dissipation Factor, 10 GHz	MIL-P-13949	.0012
Surface Resistivity, Ohms	D257-57T	
As received		3.0×10^{14}
96 hours, 100% R.H., 23°C		3.0×10^{14}
Volume Resistivity, Ohm - Cm		
As received		2.0×10^{13}
96 hours, 100% R.H., 23°C		2.0×10^{13}
Arc Resistance	D495-56T	No track up to melting at 180 seconds

*Typical test values taken at 73°F except where otherwise noted.

6/70
Superseding 3/69

HEWLETT hp PACKARD

COMPONENTS

SILICON IMPATT* DIODES 5-14 GHz

Model 5082-0430 Series

TECHNICAL DATA SHEET SEPT. 1971

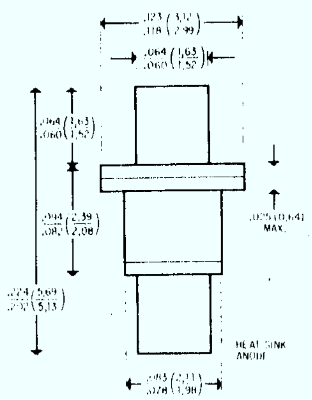

HP Package Style 31

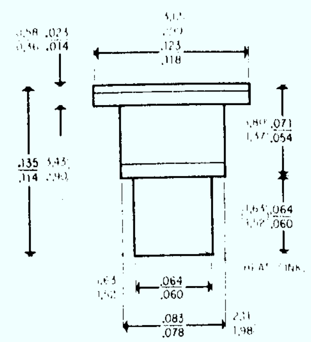

HP Package Style 41

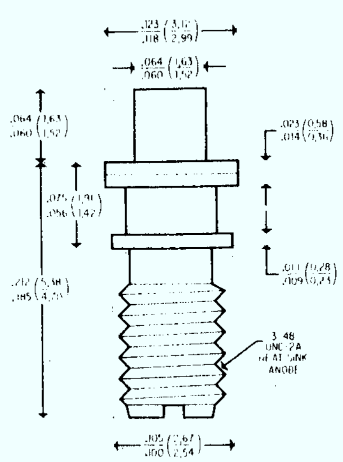

HP Package Style 62

Features

- **Low Cost**
  Achieved by unique batch fabrication process
- **Optimized for Consumer and Industrial Equipment requiring 10-150 mW**
- **High Reliability**
  $T_j < 150^\circ C$ @ 100 mW and $T_A = 50^\circ C$
- **Low Thermal Resistance**
  Typical $30^\circ C/W$
- **Low Noise**
  AM: Typ. – 135 dB in 100 Hz BW, 1 kHz from carrier
  FM: Typ. 3 Hz (RMS) in 100 Hz BW, 1 kHz from carrier
  $Q_{EXT} = 2400$

General Description

* IMPATT (IMPact Ionization Avalanche Transit Time) diodes are junction devices operated with reverse bias sufficient to cause avalanche breakdown (typical 70-115 V, 20-40 mA). In this device, the combination of avalanche generation and drift of carriers across the diode's active region produces negative resistance at microwave frequencies. Thus, in the appropriate circuit, the device can be the active element of a microwave oscillator or microwave amplifier.

Applications

Devices of the 5082-0430 series are optimized for consumer and industrial applications requiring a low cost oscillator diode for the frequency range 5-14 GHz. The devices operate in a properly adjusted cavity as a 100 mW oscillator with high efficiency and a high level of inherent device reliability. Typical applications consist of intrusion alarm radars, traffic control radars, fuses, automatic braking systems and low cost telecommunications repeaters. More detailed information is available in HP Application Note 935.

Device Construction

HP 5082-0430 series IMPATT diodes are silicon mesa p-n junction devices fabricated using low temperature, double epitaxial techniques. This process assures abrupt junctions and exact control of the thickness of the active portion of the device. Heat sinking of the diode is provided by an integral heat sink which is batch-fabricated using an HP unique manufacturing process for uniformity, economy, and intimate thermal contact between the junction and the heat-carrying metal.

Absolute Maximum Ratings:

Parameter	Symbol	5082-0430 Series
Storage Temperature	T_{STG}	150°C
Junction Operating Temperature (Note 6)	T_J	200°C
Power Dissipation (Note 7)	P_{DISS}	$\frac{200 - T_{CASE}}{\theta_{JC}}$

Electrical Specifications at T_A=25°C:

Parameter	Symbol	5082-0431 5082-0434 5082-0437	5082-0432 5082-0435 5082-0438	5082-0433 5082-0436 5082-0439	Units	Notes
Frequency Range	f	5-9	8-12	10-14	GHz	–
Minimum CW Output Power	P_O		100		mW	1
Maximum Thermal Resistance	θ_{JC}		35		°C/W	2

Typical Parameters at T_A=25°C:

Parameter	Symbol	5082 -0431	5082 -0432	5082 -0433	5082 -0434	5082 -0435	5082 -0436	5082 -0437	5082 -0438	5082 -0439	Units	Notes
HP Package Style No.	–		41			62			31		–	–
Operating Voltage	V_{OPR}	110	90	75	110	90	75	110	90	75	V	9
Operating Current	I_{OPR}	25	30	35	25	30	35	25	30	35	mA	9
Breakdown Voltage	V_{BR}	103	78	65	103	78	65	103	78	65	V	3
Junction Capacitance at V_{BR} (±20%)	$C_j(V_{BR})$	0.29	0.20	0.30	0.29	0.20	0.30	0.29	0.20	0.30	pF	4
Typical Efficiency	η					3.5					%	5
Typical Package Capacitance	–		.30			.30			.26		pF	–
Typical Package Inductance	–		.60			.60			1.0		nH	8

Mechanical Specifications

Hewlett-Packard's Impatt Diodes are presently available in the HP Style 31, 41 and 62 packages. However, a variety of packages are available upon request. Contact your local HP field office for additional information.

The metal-ceramic package is hermetically sealed. The cathode stud and flange is gold-plated Kovar. The anode stud is gold-plated copper. The maximum soldering temperature for a metal ceramic package is 235°C for 5 seconds.

NOTES:

1. Output power is measured in a nominally fixed-tuned mount with Q_{EXT} = 40 and P_{IN} (max) = 3.5 W.
2. R. H. Haitz, IEEE Transactions, ED - 16, 1969 pp. 438-444.
3. I_R = .5 mA.
4. Measured at 1.0 MHz.
5. $\eta = P_O/P_{IN}$.
6. Diode burnout occurs for $T_J \simeq 350$°C. Operation at $T_J < 200$°C thus allows a large margin for safety, ensuring long-term reliable operation and stability of diode parameters.
7. $P_{DISS} = P_{IN} - P_O$.
8. Measured in X-band in 0.276" O.D. coaxial transmission line. Diode biased to $V = V_{BR}$.
9. IMPATT devices are operated under reverse bias, requiring that the negative terminal of the dc power supply go to the anode (heat sink).

PRINTED IN U.S.A.

5952-0242

APPENDIX B

BIAS CONSIDERATIONS FOR THE IMPATT DIODE

Since in the avalanche breakdown mode, the IMPATT diode tends to behave as a constant voltage device, it requires a constant-current DC bias source. The required constant current source may be constructed from a large resistor and a high voltage power supply. However, this method of supplying a constant current is unsatisfactory since there is a large wastage of power in the resistor. Furthermore, this method is also subject to the possibility of bias circuit oscillations resulting from stray inductance and capacitance which form a high Q series resonance circuit to ground.

A better constant current source may be obtained from a laboratory power supply and a transistor current regulator circuit. Such a circuit design is described in reference 36. This circuit has been adapted for use in the experimental work in this thesis as shown in figure B1. Each diode in the two-device circuit configurations described in chapter 3 were biased by an individual current regulator circuit.

APPENDIX C

TESTBED DESCRIPTION AND CALIBRATION

The testbed upon which all the circuits described in this thesis were tested is shown as a block diagram in figure C1. Except for the constant current regulator circuit, all the testbed components are standard laboratory equipment.

The testbed was characterized with respect to VSWR and attenuation over the frequency range of 9.5 to 10.5 GHz. The maximum VSWR, as measured by a Hewlett-Packard 8410S Network Analyzer system, was 1.32 (0.081 dB transmission loss). Results for the total transmission loss through the testbed are given in figure C2. These results were obtained by using a Hewlett-Packard, model 8690A, sweep oscillator as the signal source and monitoring (via a bolometer and power meter) both its power output, and that of the testbed on an X-Y recorder. Over the frequency range, the average attenuation in the testbed was 1.0 dB, within an accuracy of ± 0.15 dB. This value was used as a correction factor for the power meter readings reported in this thesis.

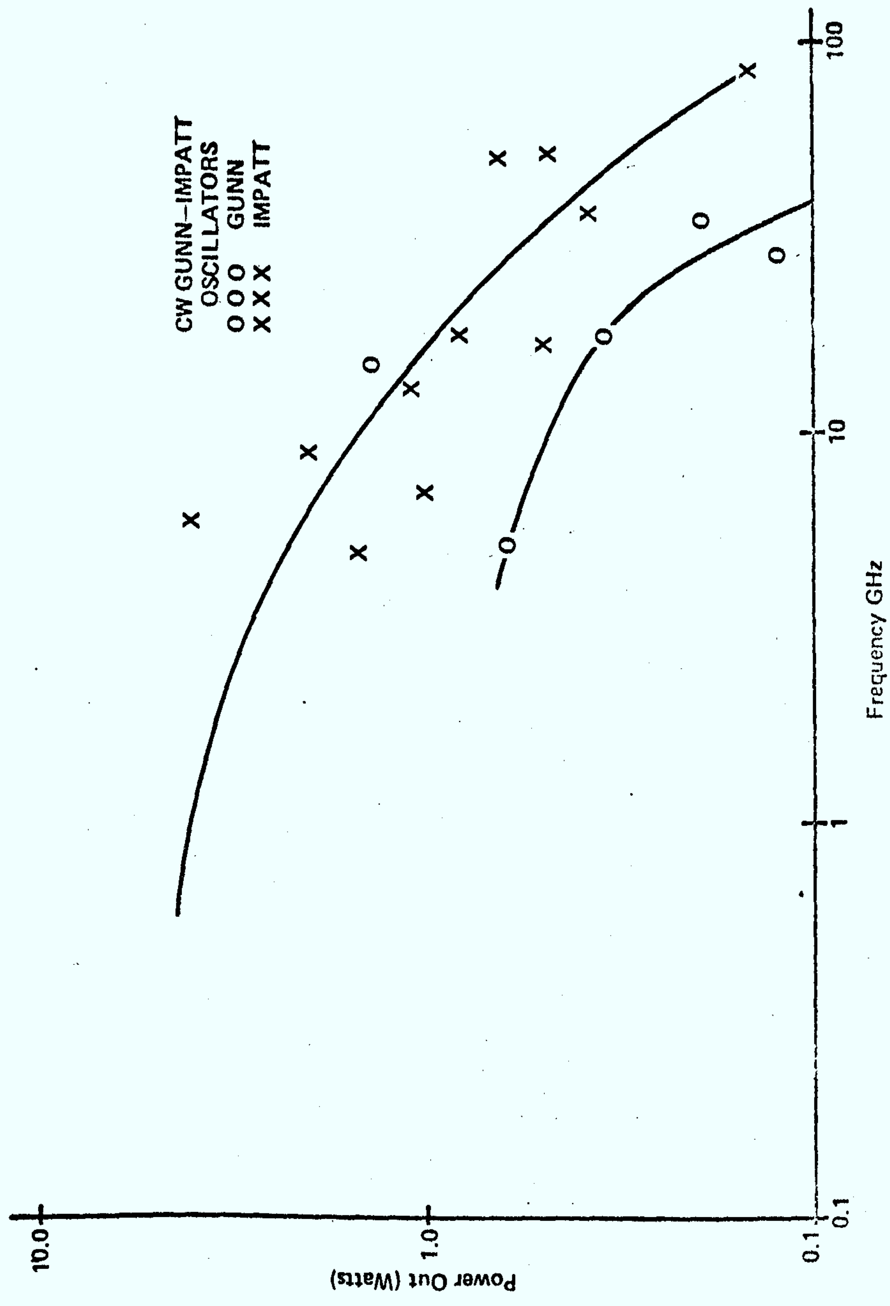

Figure I.I: Summary of the "State of the Art" in Single-device Two-Terminal Solid-State, Microwave Sources(I)

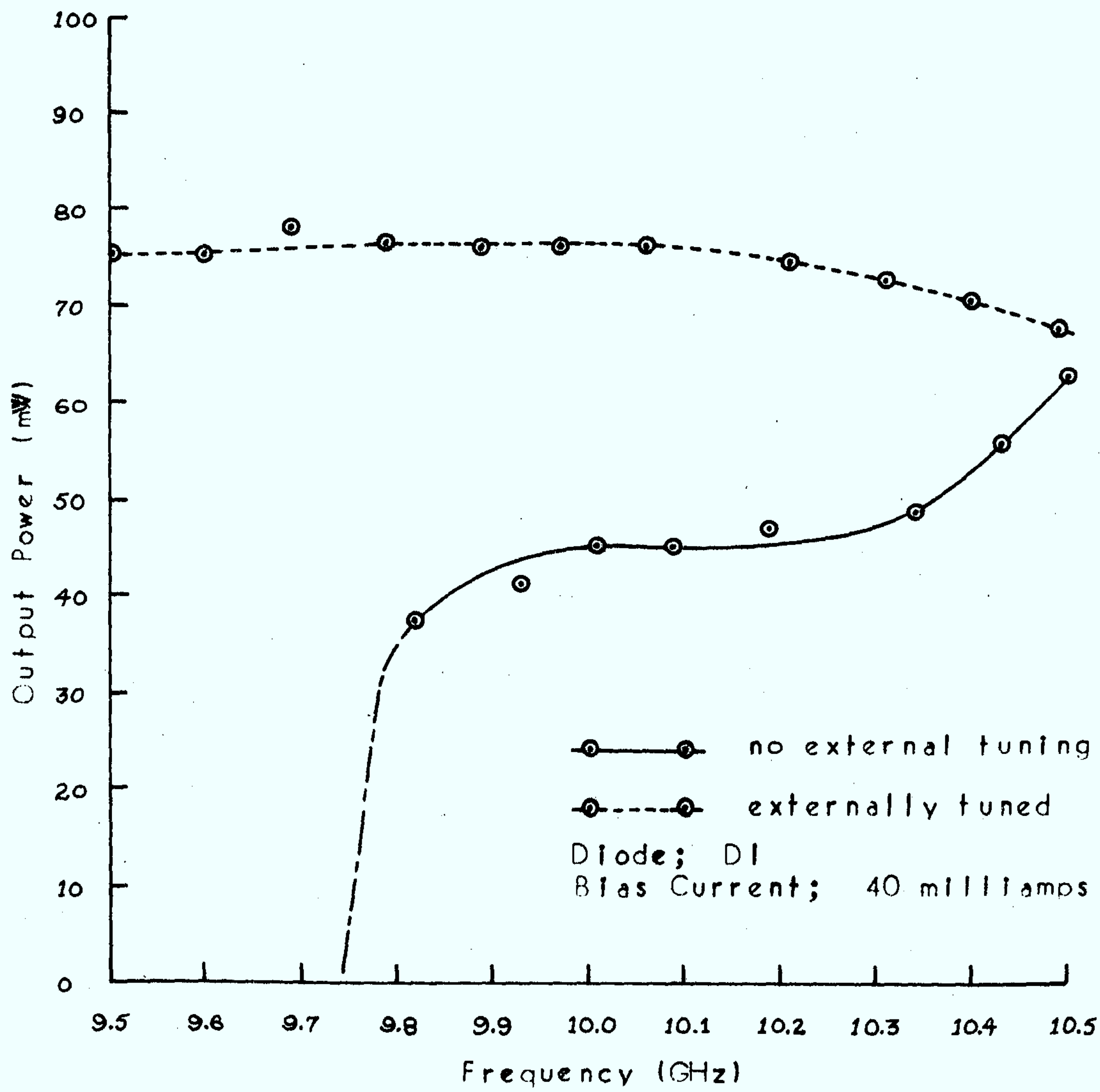

Figure 2.1; Experimental Determination of the Parasitic Load Conductance g_l (g_l assumed to be 0 millimhos)

(Results corrected for testbed losses - see Appendix C)

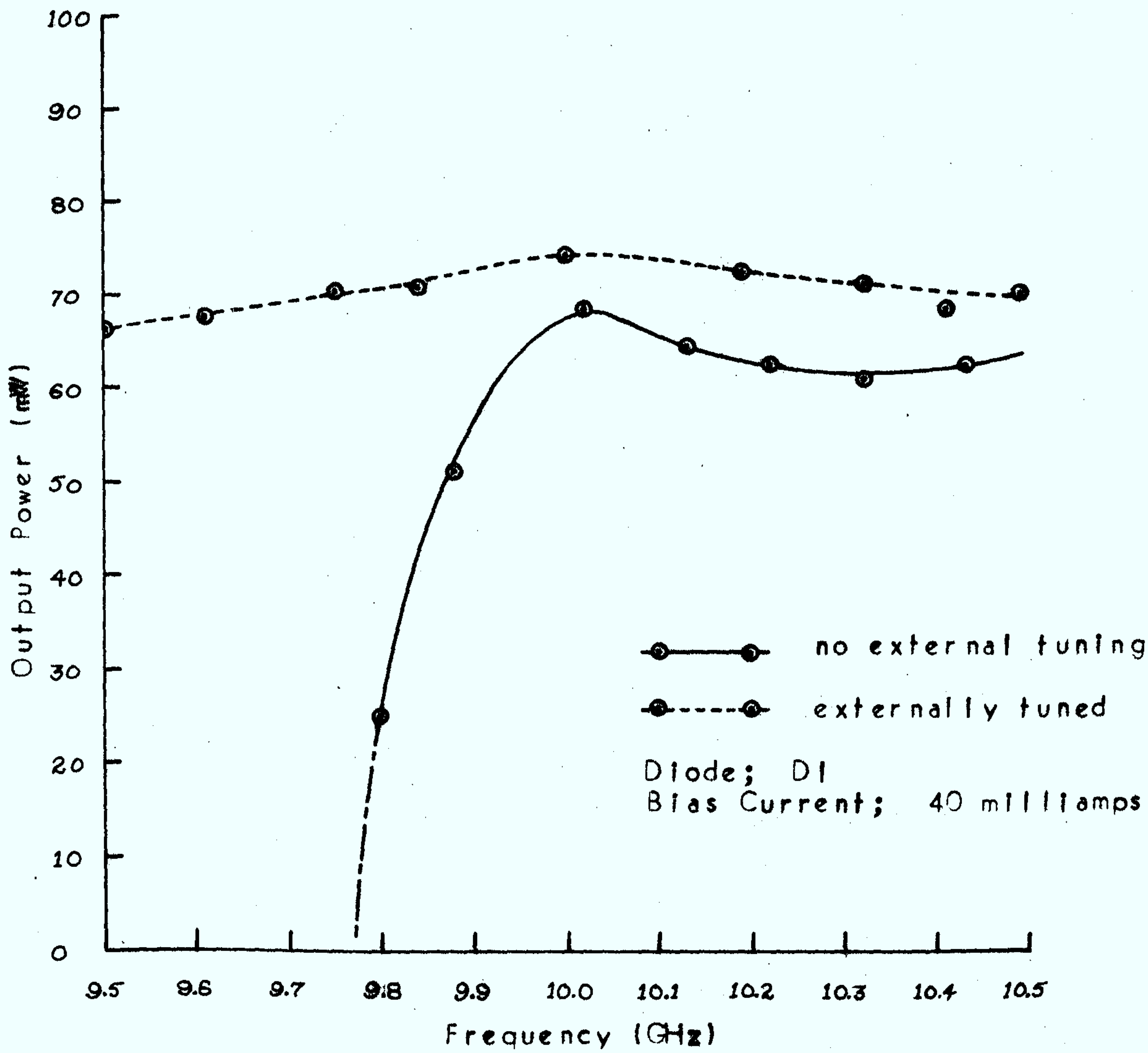

Figure 2.2; Experimental Determination of the Parasitic Load Conductance g_l (g_l assumed to be 0.5 millimhos)

(Results corrected for testbed losses - see Appendix C)

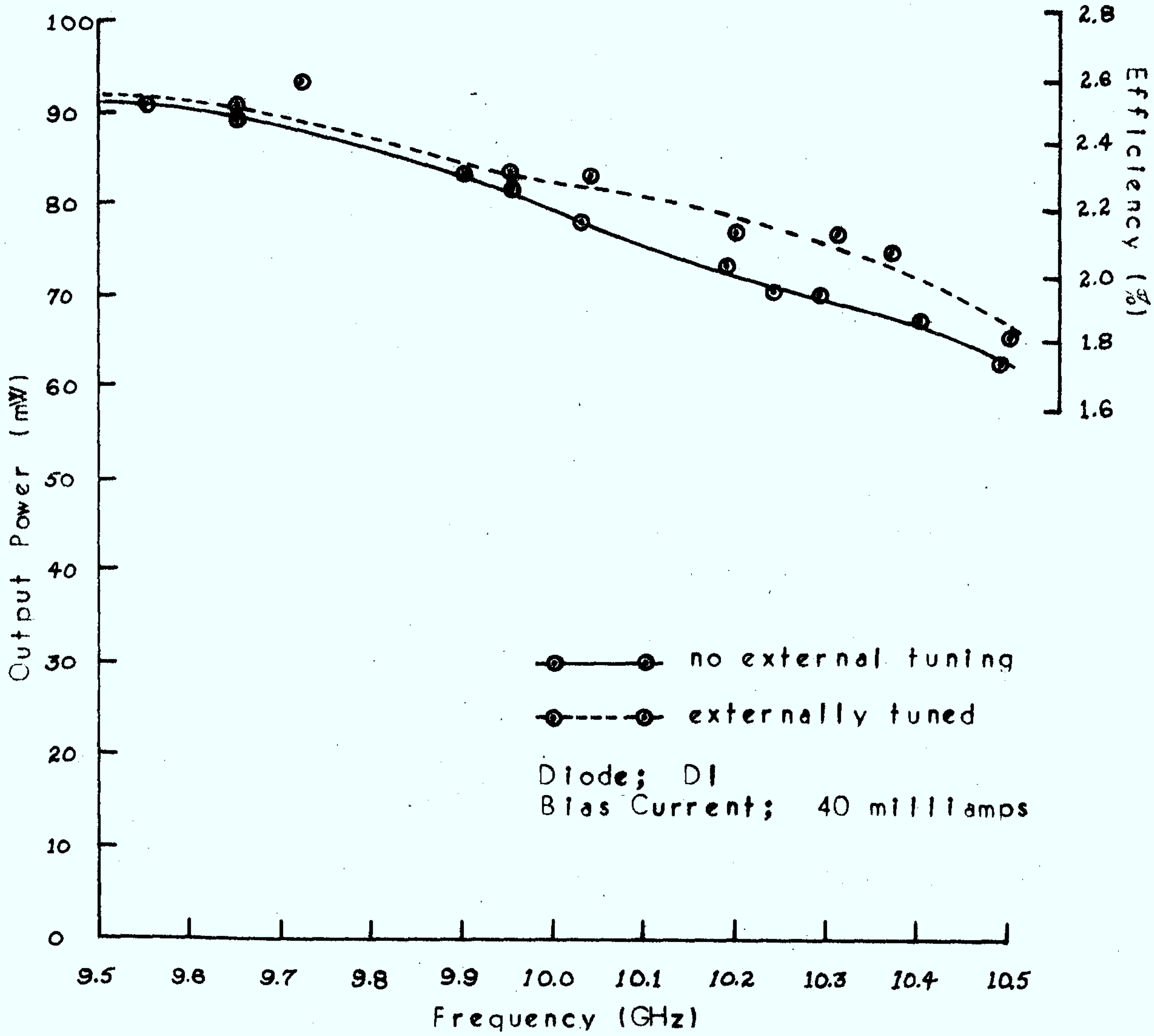

Figure 2.3; Experimental Determination of the Parasitic Load Conductance g_L (g_L assumed to be 1.0 millimhos)

(Results corrected for testbed losses - see Appendix C)

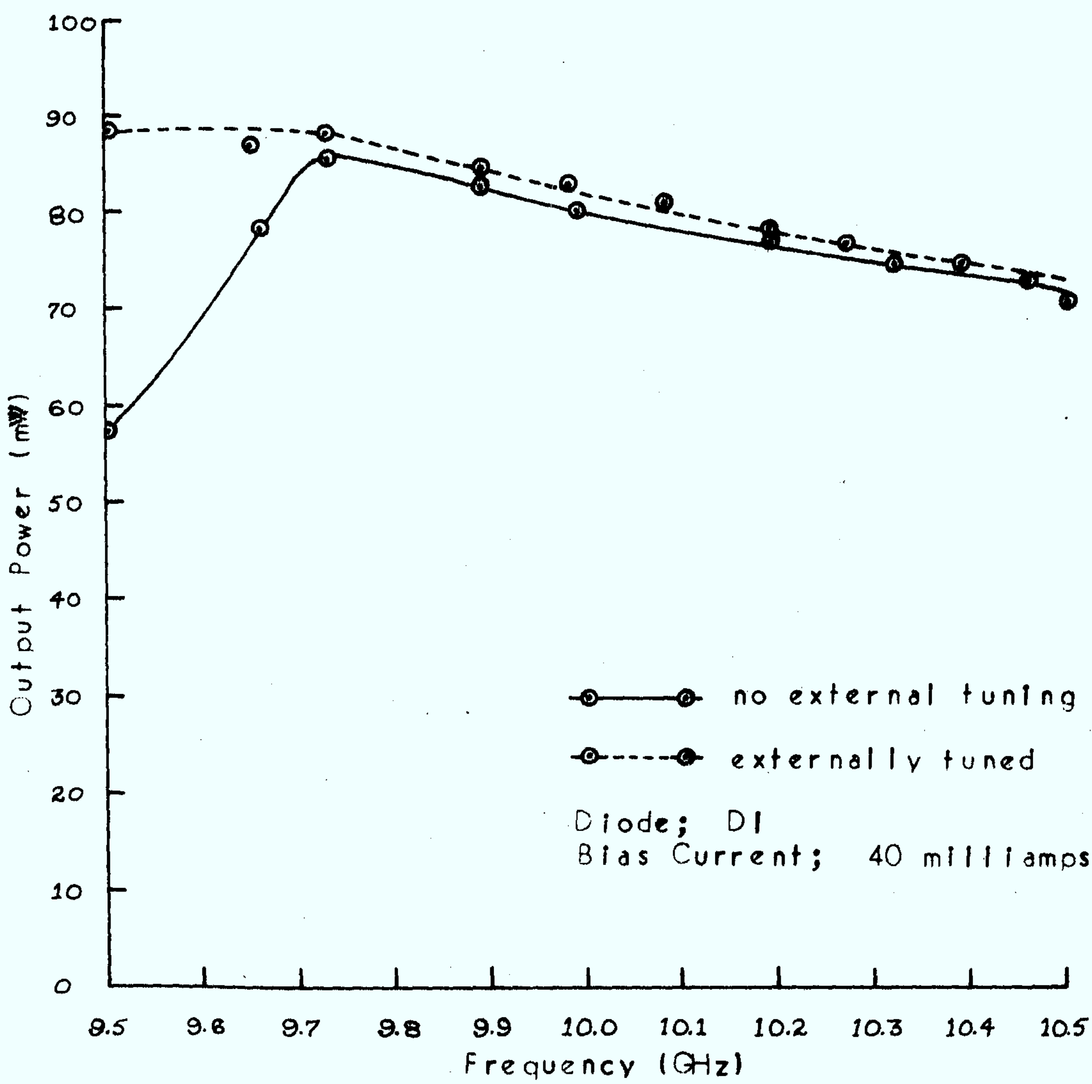

Figure 2.4; Experimental Determination of the Parasitic Load Conductance g_L (g_L assumed to be 1.5 millimhos)

(Results corrected for testbed losses - see Appendix C)

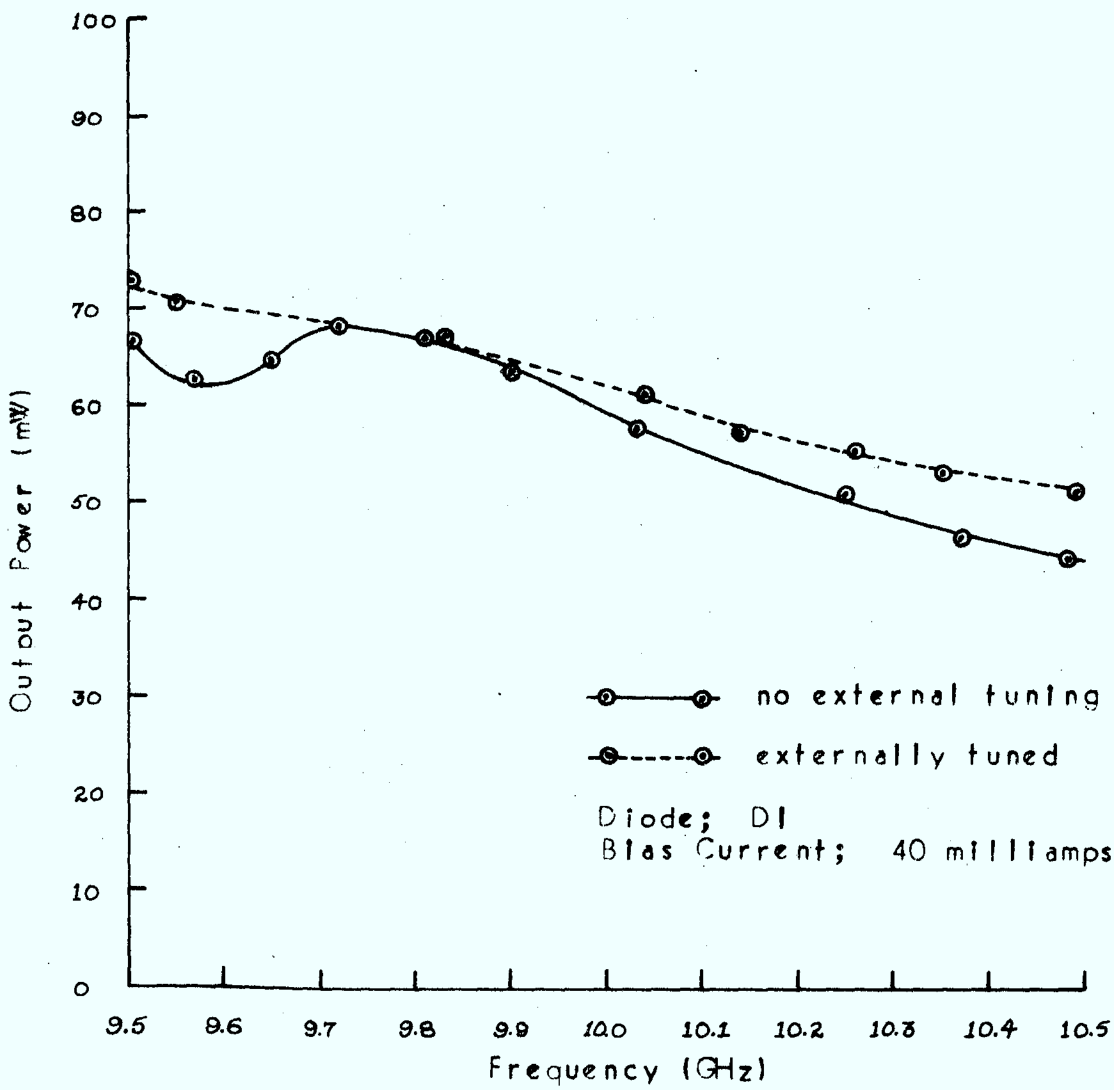

Figure 2.5: Experimental Determination of the Parasitic Load Conductance g_L (g_L assumed to be 2.0 millimhos)

(Results corrected for testbed losses - see Appendix C)

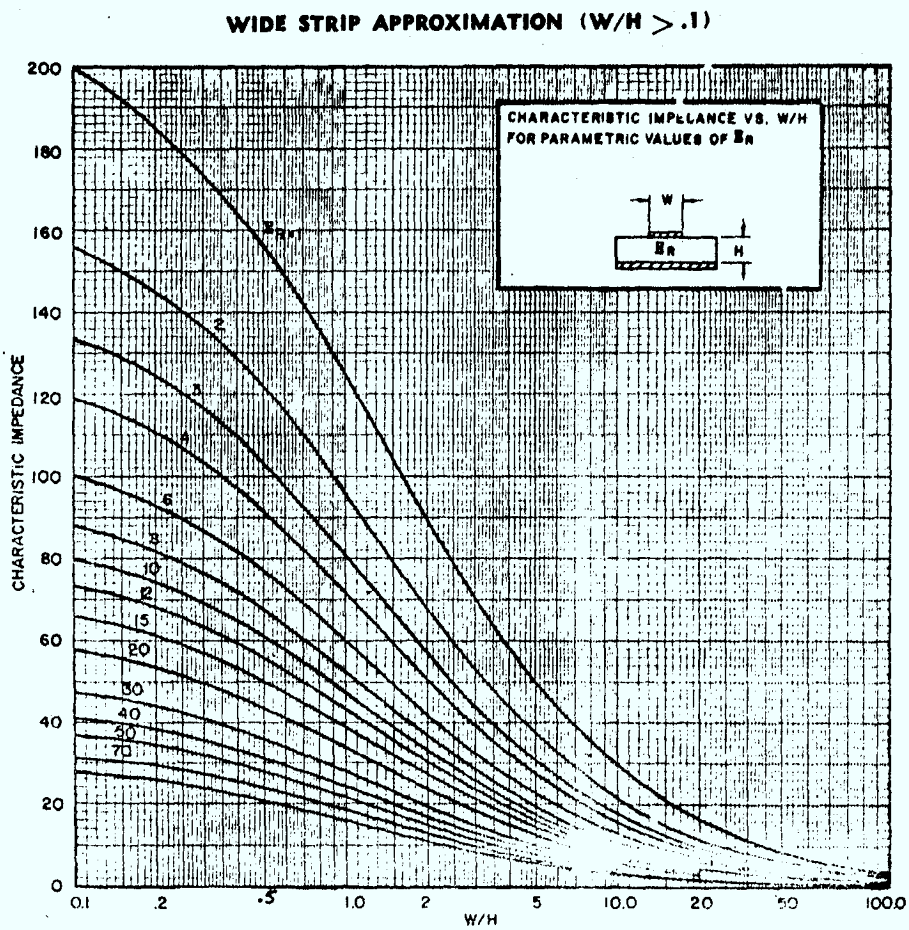

Figure 2.6a; Microstrip Transmission Line Characteristic Impedance vs. W/h for Parametric Values of ϵ_r - Wide Strip Approximation (Wheeler's Curves)(28)

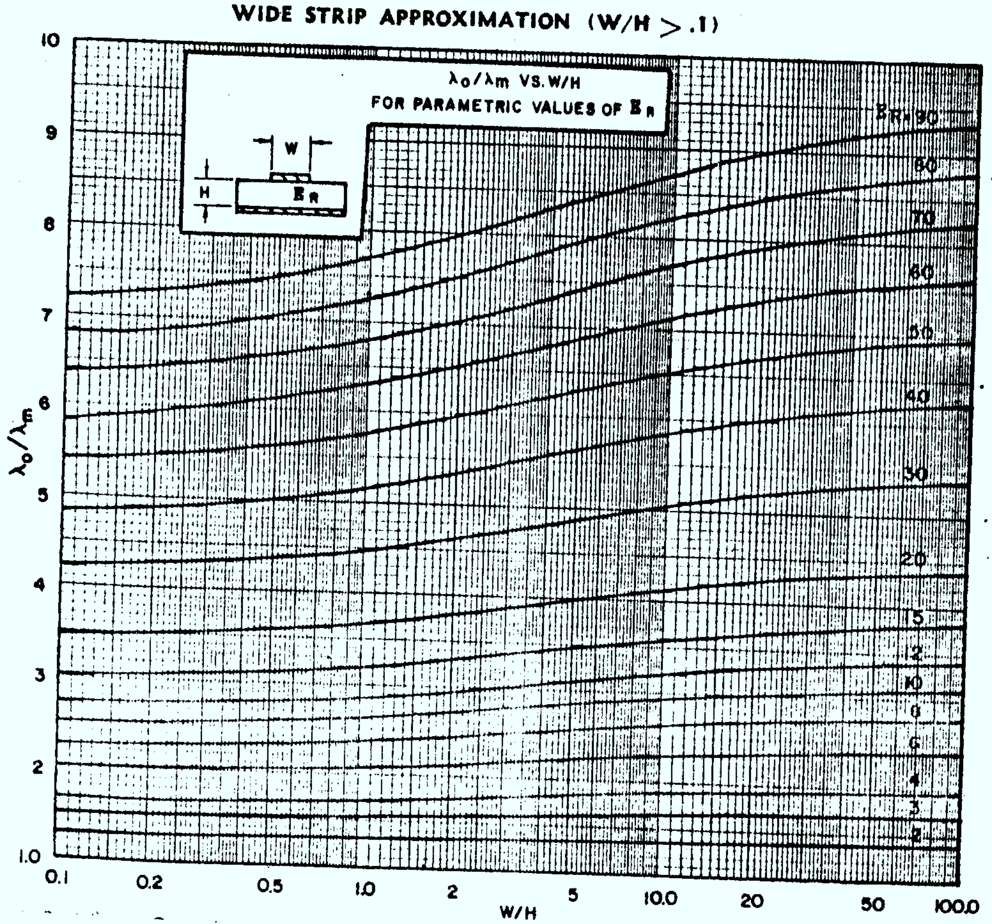

Figure 2.6b; λ_o/λ_m vs W/h for Parametric Values of ϵ_r - Wide Strip Approximation (Wheeler's Curves)(28)

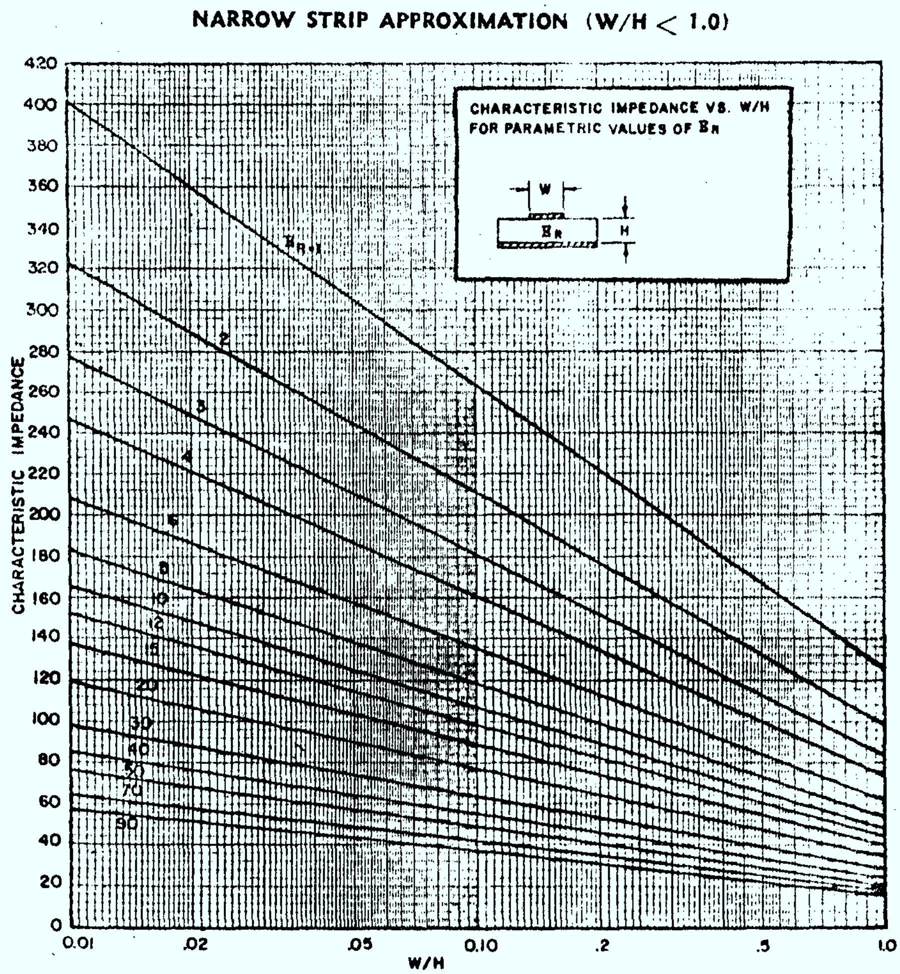

(Figure 2.6c; Microstrip Transmission Line Characteristic Impedance vrs $^{w}/_{h}$ for Parametric Values of ϵ_r - Narrow Strip Approximation (Wheeler's Curves)[28]

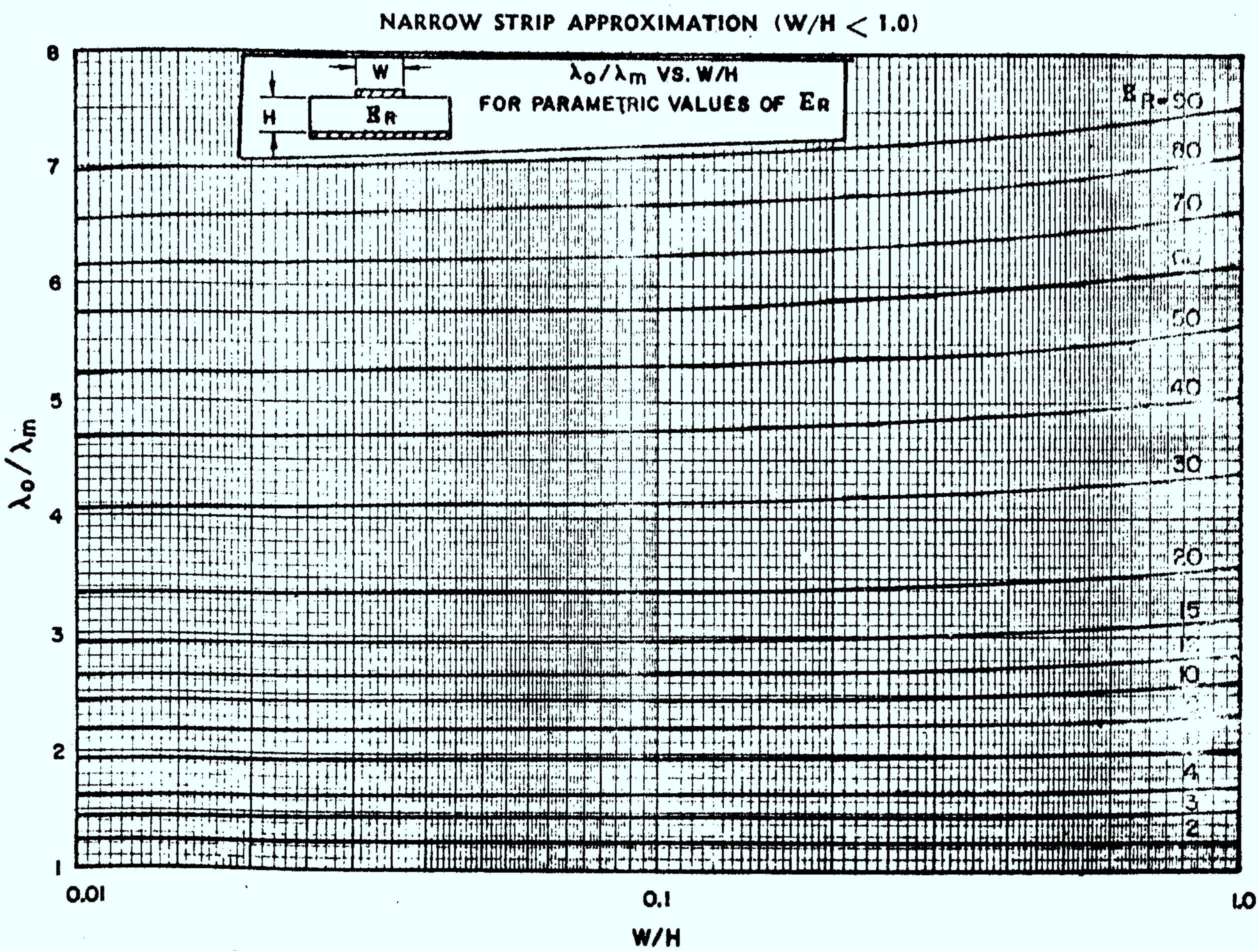

Figure 2.6d; λ_o/λ_m vs. W/h for Parametric Values of ϵ_r — Narrow Strip Approximation (Wheeler's Curves)(28)

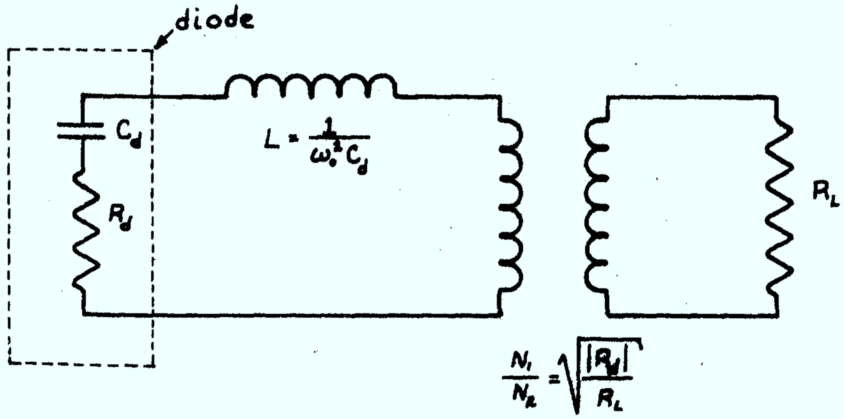

Figure 2.7a; Series Equivalent Circuit Load Configuration

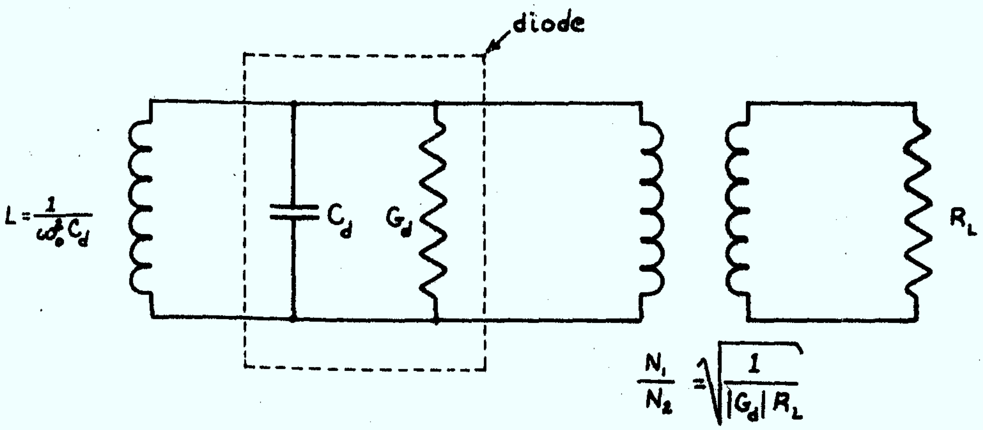

Figure 2.7b; Parallel Equivalent Circuit Load Configuration

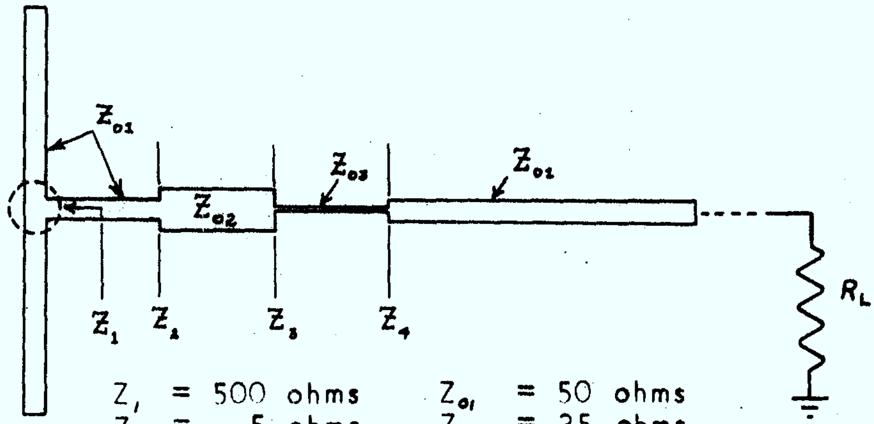

Z_1	=	500 ohms	Z_{01}	=	50 ohms
Z_2	=	5 ohms	Z_{02}	=	35 ohms
Z_3	=	245 ohms	Z_{03}	=	110.7 ohms
Z_4	=	50 ohms	R_L	=	50 ohms

Figure 2.8a; Design Impedance Values for Circuit Configuration AI

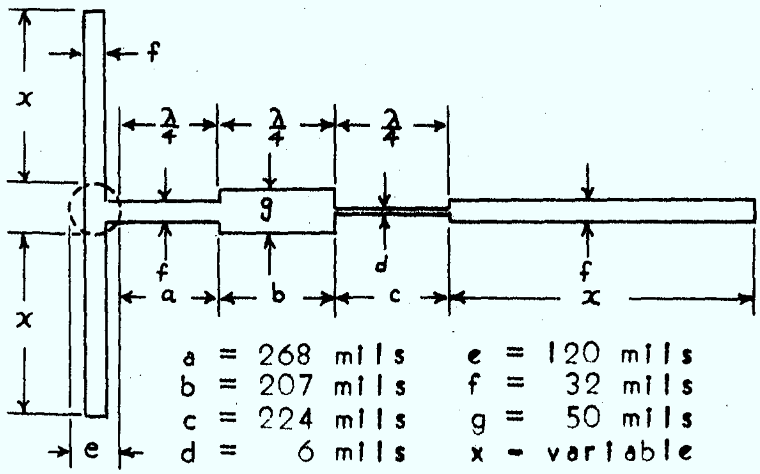

a	=	268 mils	e	=	120 mils
b	=	207 mils	f	=	32 mils
c	=	224 mils	g	=	50 mils
d	=	6 mils	x	-	variable

Figure 2.8b; Dimensions of Circuit Configuration AI

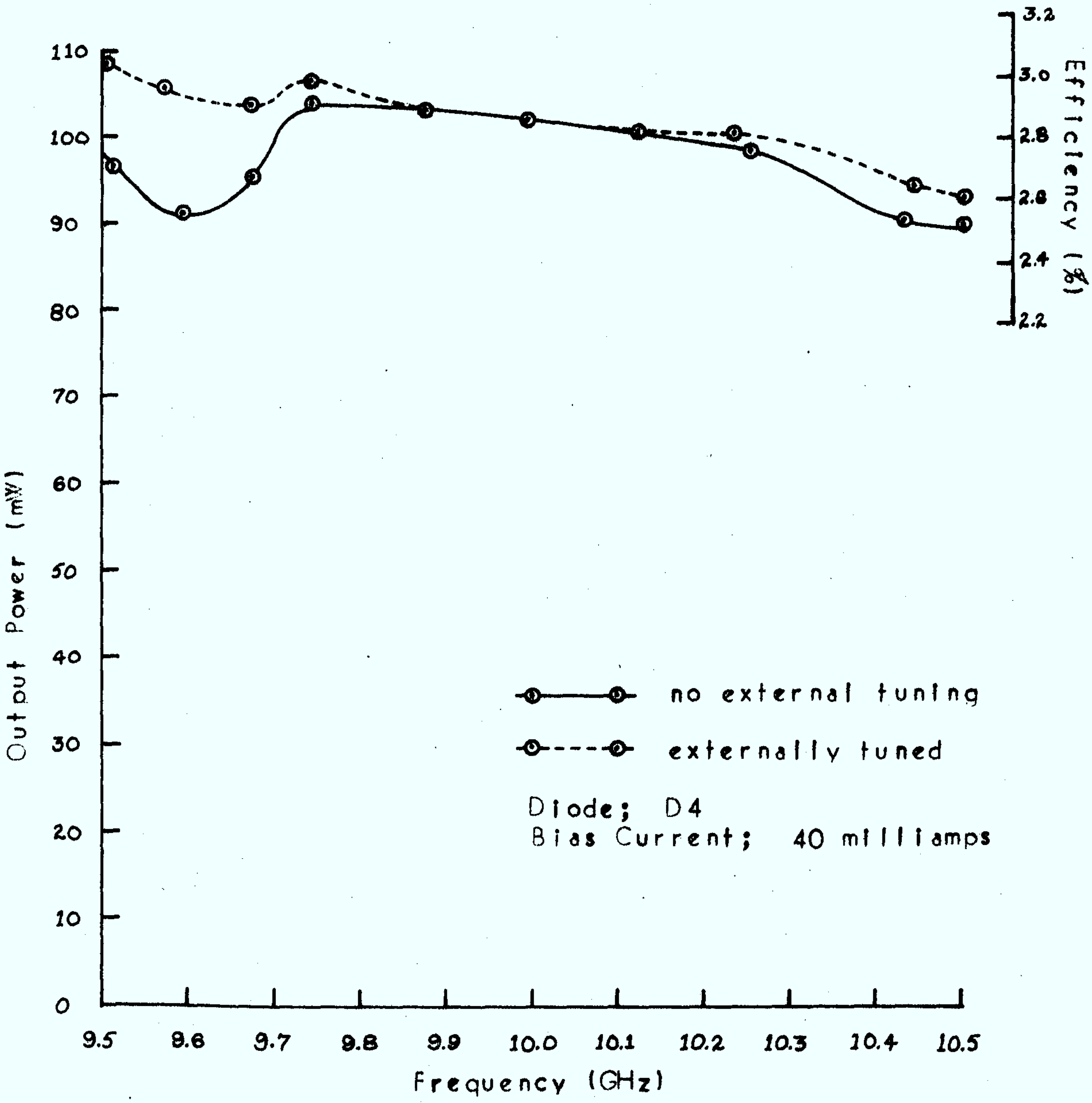

Figure 2.9; Output Power and Efficiency vs Frequency for Circuit Configuration A1. (Results corrected for testbed losses - see Appendix C)

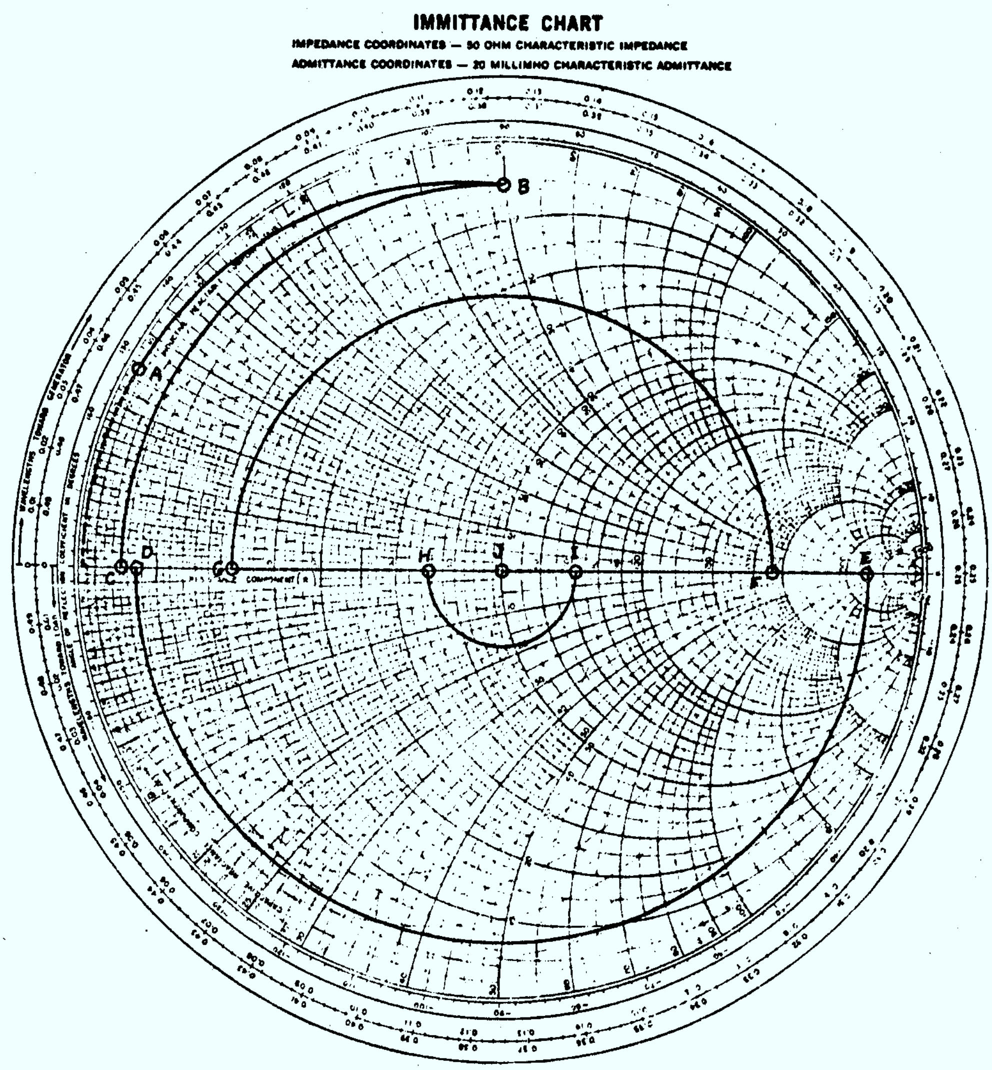

Figure 2.10; Design Philosophy of Circuit Configuration A2.

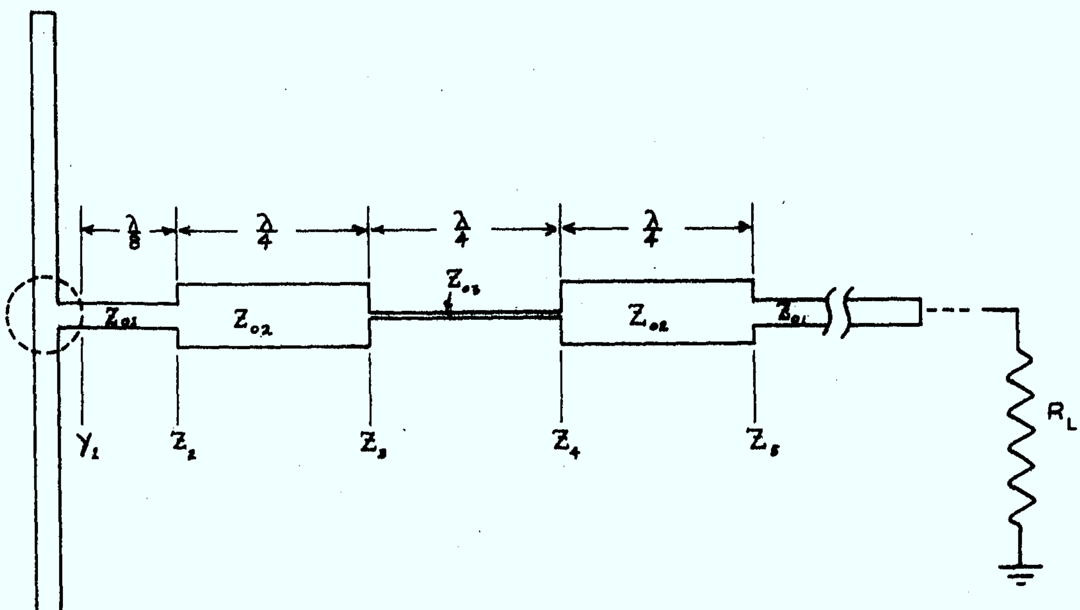

Y_1 = 2-j20 millimhos
Z_2 = 2.5 ohms
Z_3 = 490 ohms
Z_4 = 22 ohms
Z_5 = 50 ohms

Z_{01} = 50 ohms
Z_{02} = 35 ohms
Z_{03} = 104 ohms
R_L ± 50 ohms

Figure 2.11; Design Immittance Values for Circuit Configuration A2.

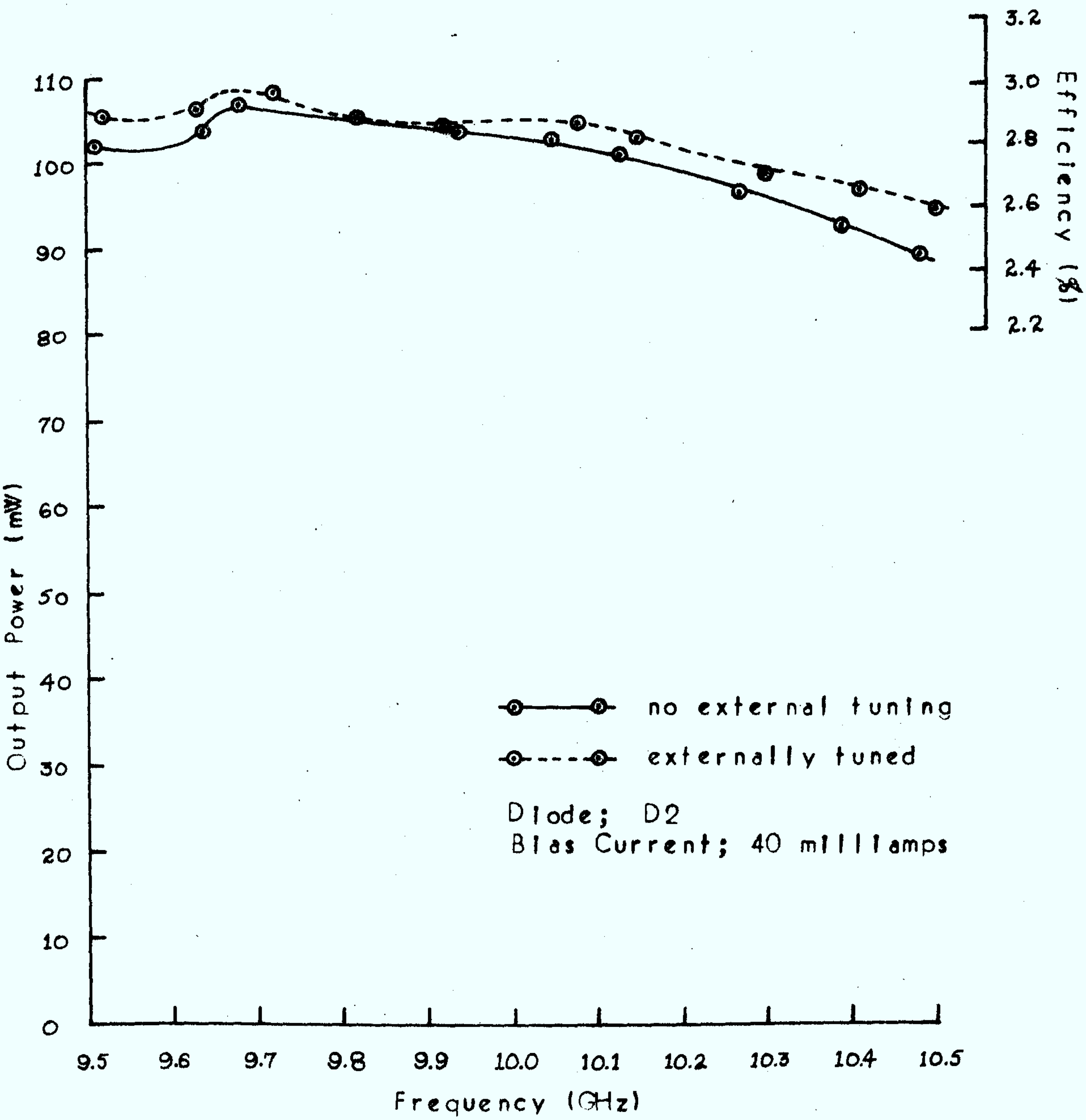

Figure 2.12; Output Power and Efficiency vs Frequency for Circuit Configuration A2 (Results corrected for testbed losses - see Appendix C)

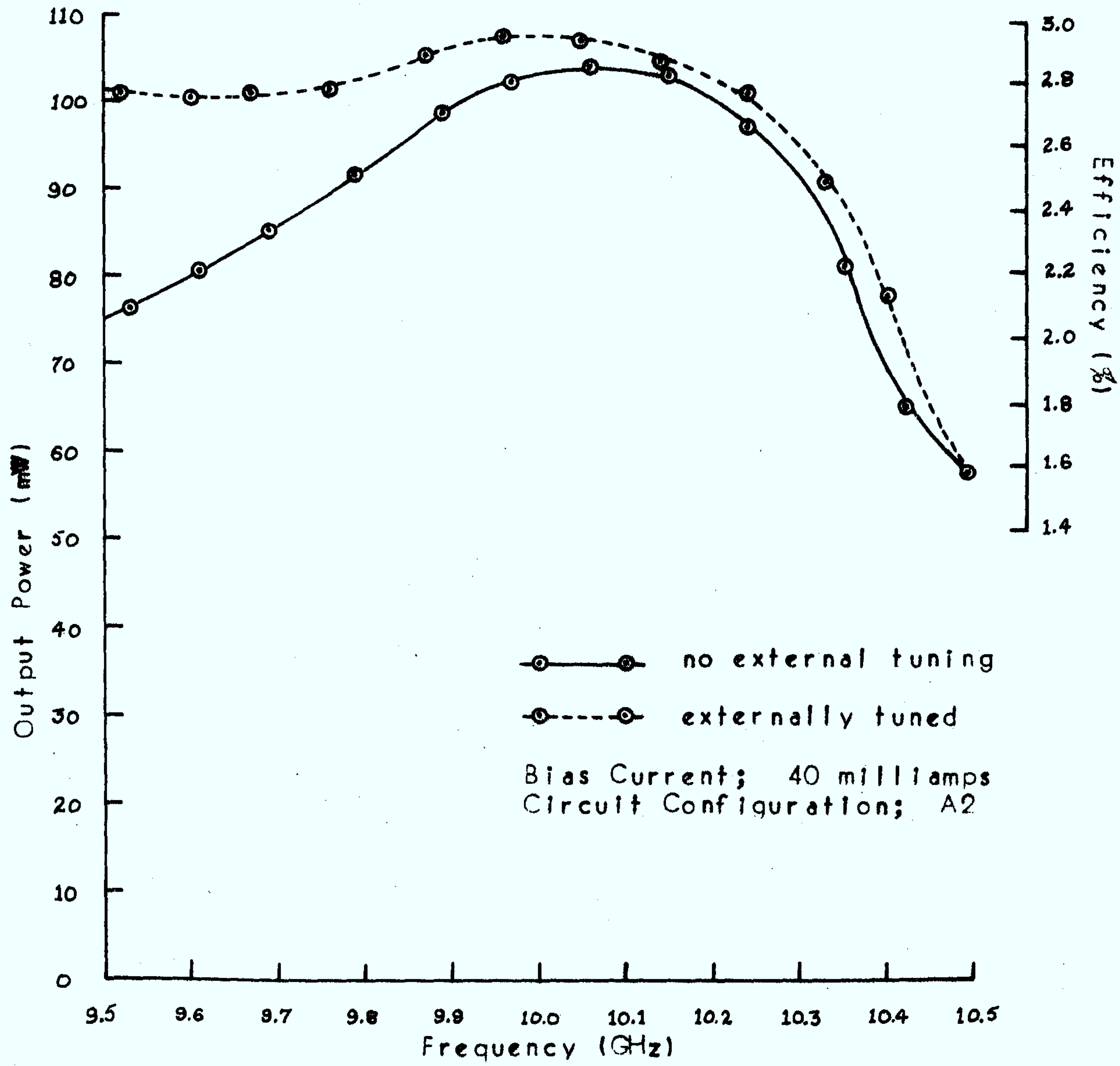

Figure 2.13; Performance of Diode D3 - Output Power and Efficiency vs Frequency

(Results corrected for testbed losses - see Appendix C)

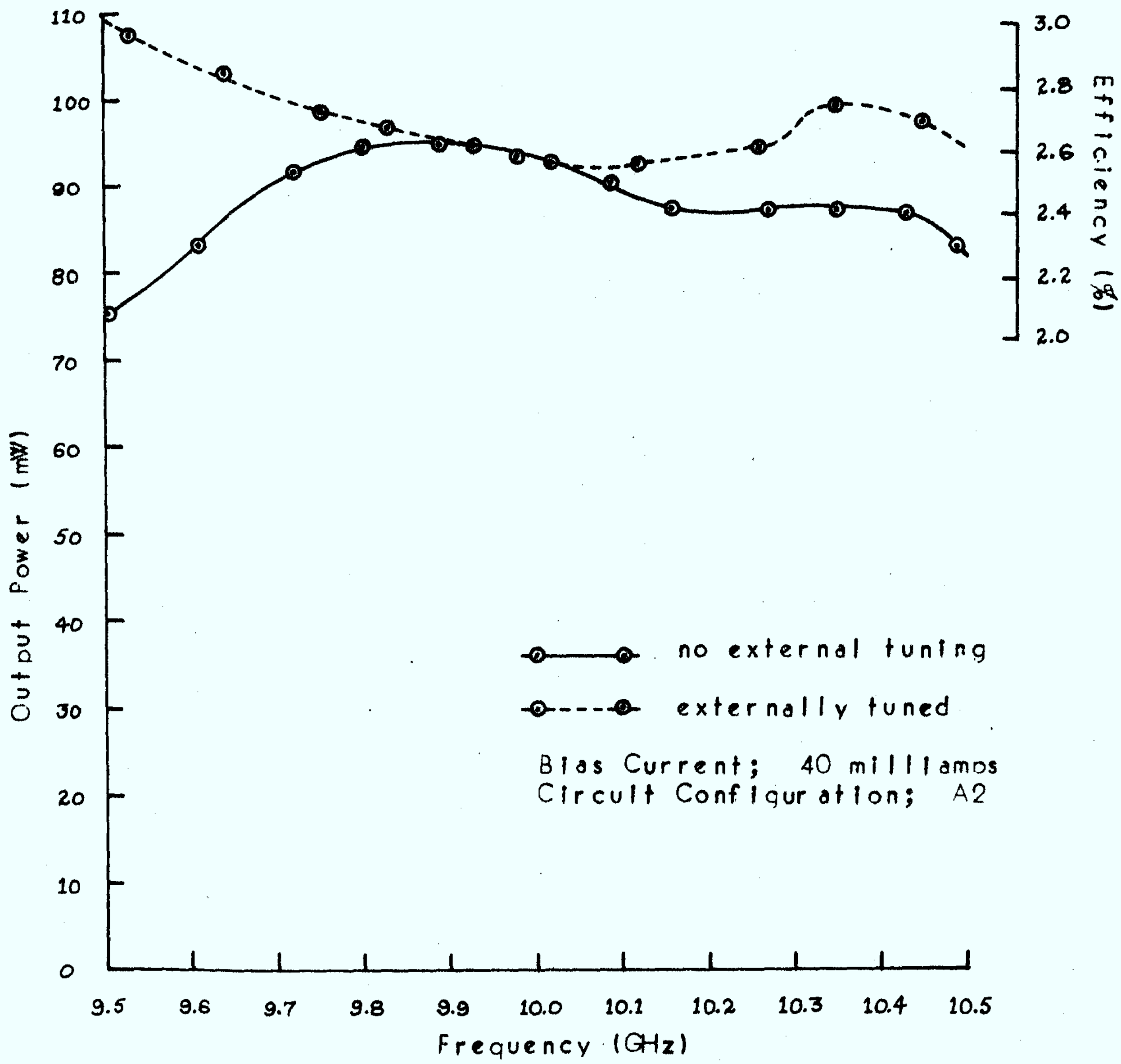

Figure 2.14; Performance of Diode D4 - Output Power and Efficiency vs Frequency

(Results corrected for testbed losses - see Appendix C)

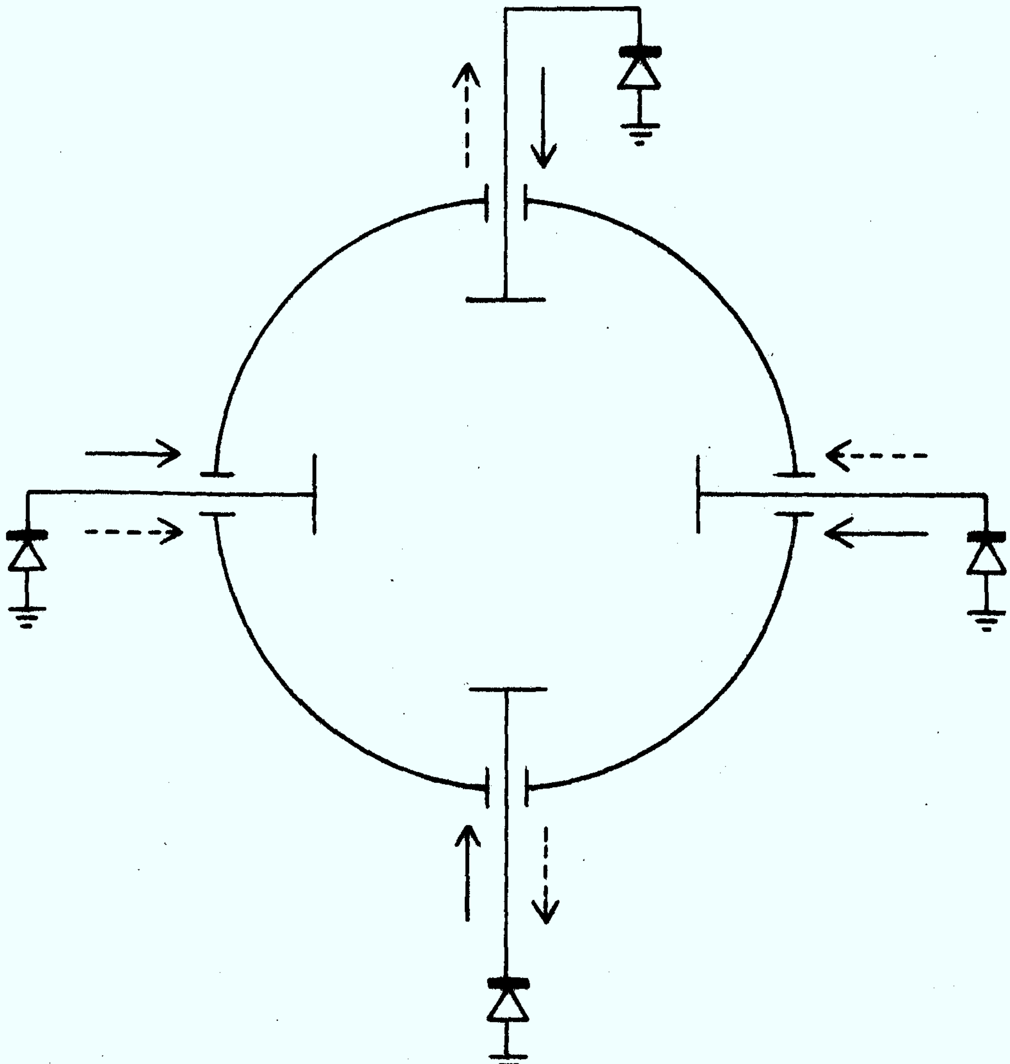

Figure 3.1: RF Current Relationships for Two Possible Modes of Oscillation in a Multiple-Device Oscillator

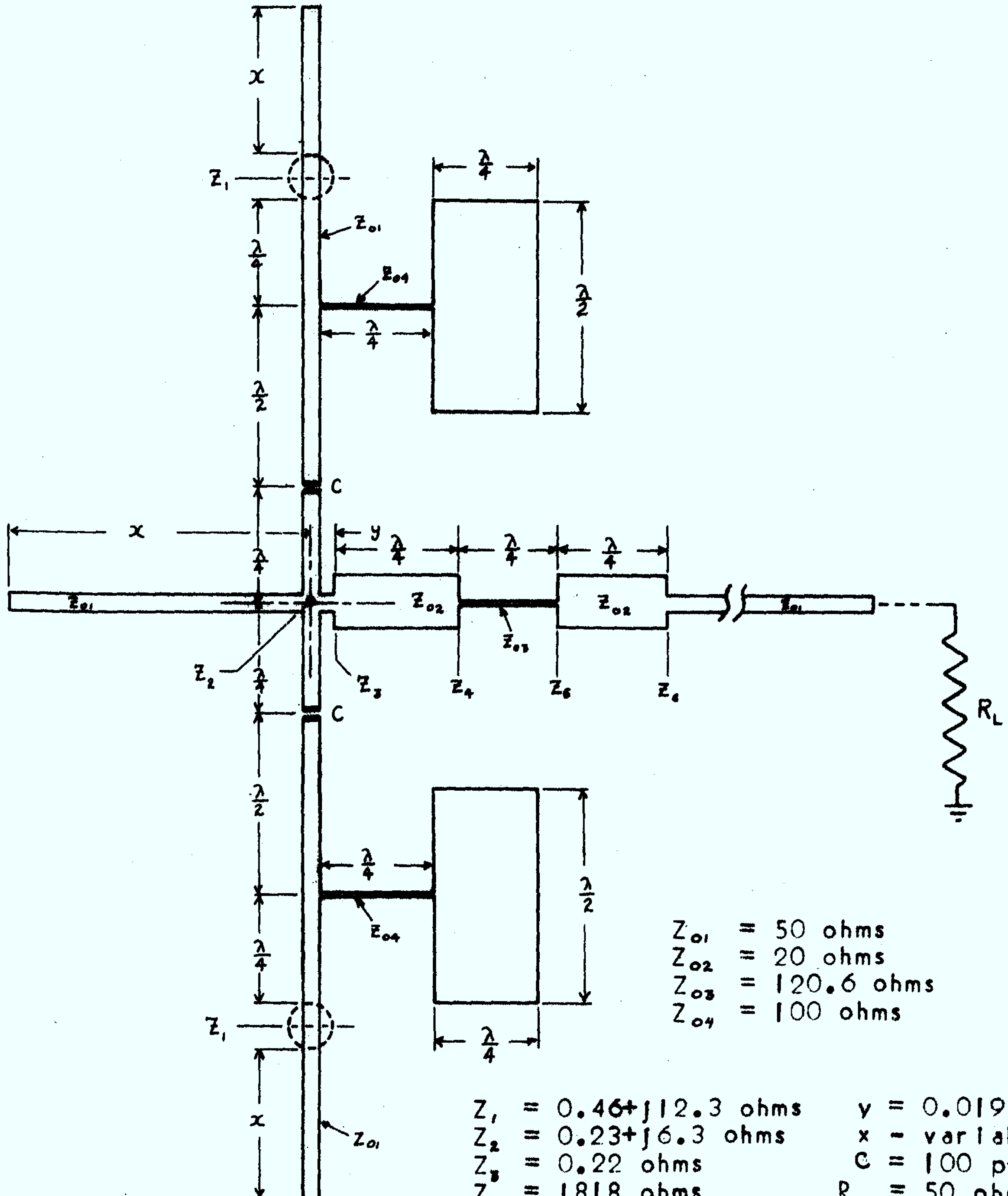

Z_{01} = 50 ohms
Z_{02} = 20 ohms
Z_{03} = 120.6 ohms
Z_{04} = 100 ohms

Z_1 = 0.46+j12.3 ohms
Z_2 = 0.23+j6.3 ohms
Z_3 = 0.22 ohms
Z_4 = 1818 ohms
Z_5 = 8 ohms
Z_6 = 50 ohms

y = 0.0198
x - variable
C = 100 pf
R_L = 50 ohms

Figure 3.2: Circuit Layout and Design Impedance Values for Circuit Configuration B1.

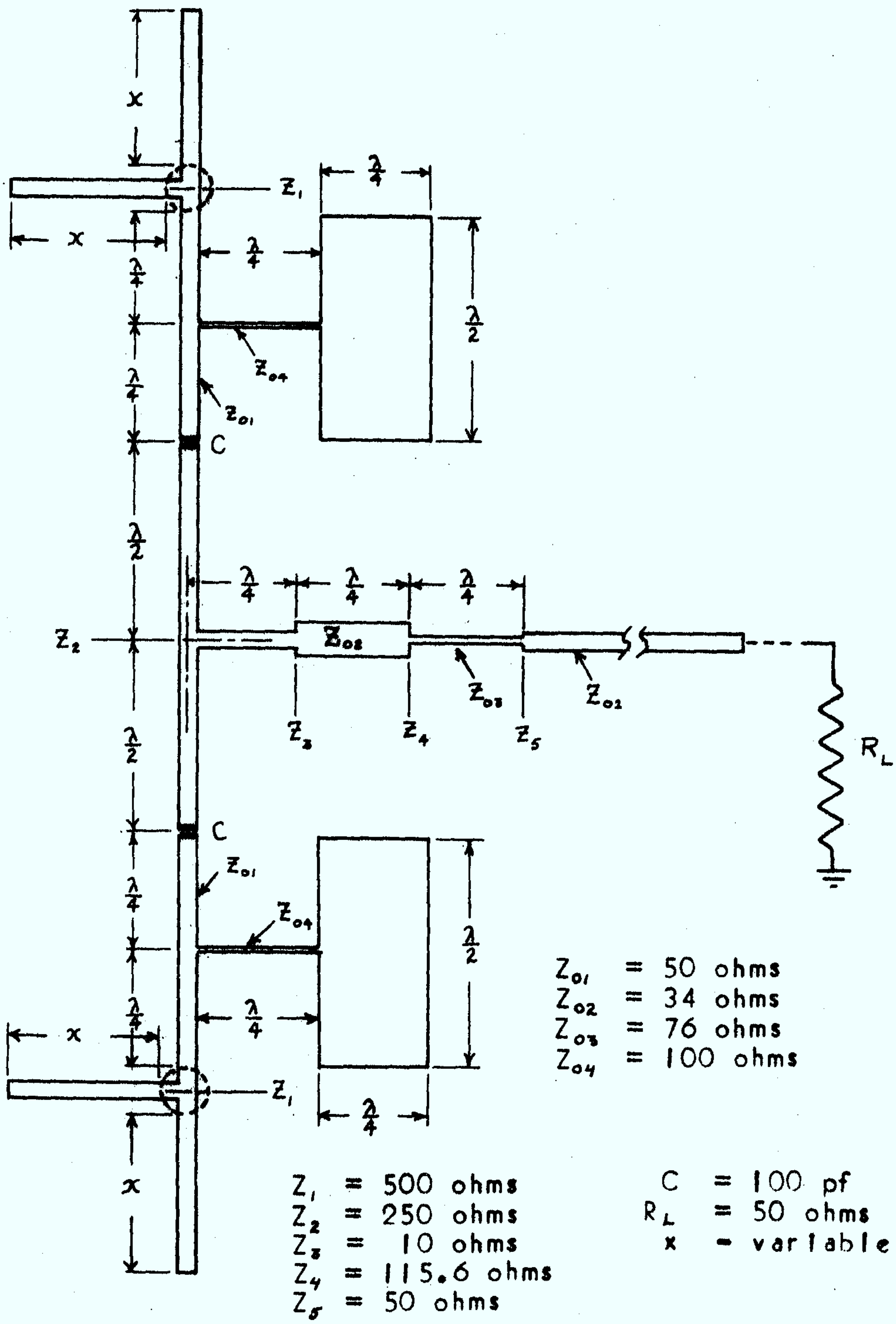

Figure 3.3 Circuit Layout and Design Impedance Values for Circuit Configuration B2

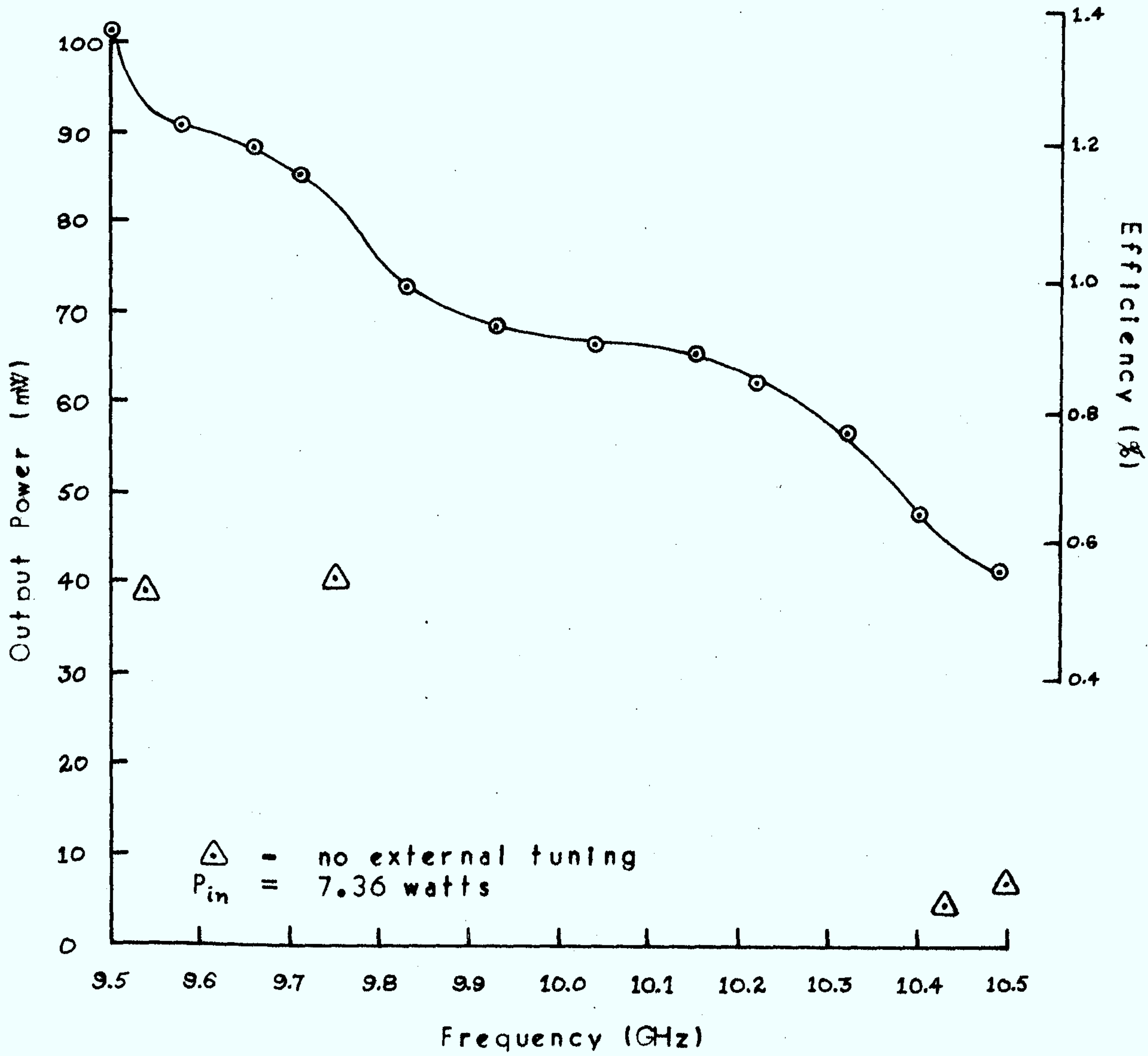

Figure 3.4: Output Power and Efficiency vs Frequency for Circuit Configuration B2

(Results corrected for testbed losses - see Appendix C)

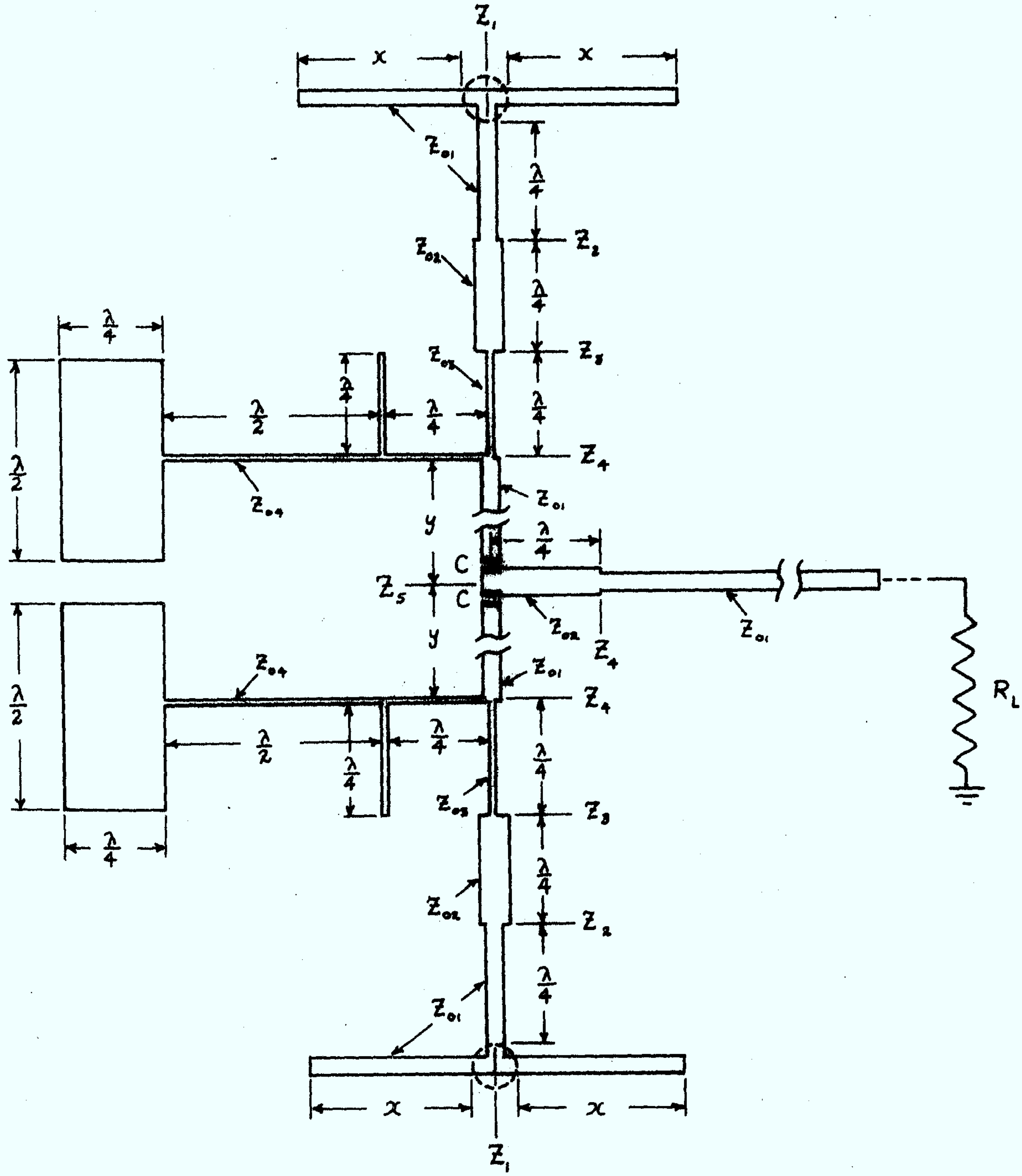

Z_{01} = 50 ohms	Z_1 = 500 ohms	C = 100 pf
Z_{02} = 35 ohms	Z_2 = 50 ohms	R_L = 50 ohms
Z_{03} = 110.7 ohms	Z_3 = 245 ohms	x - variable
Z_{04} = 104 ohms	Z_4 = 50 ohms	y: $\lambda/4$ - configuration B3
	Z_5 = 25 ohms	$\lambda/2$ - configuration B4

Figure 3.5; Circuit Layout and Design Impedance Values for Circuit Configurations B3 and B4

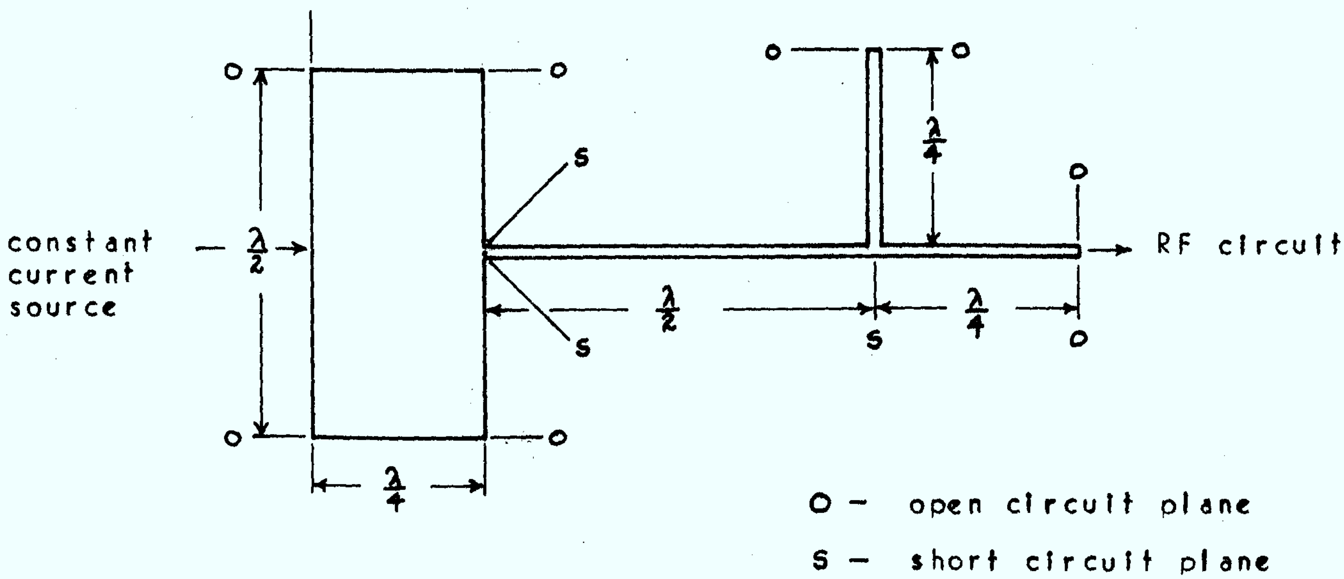

Figure 3.6; Bias Circuit Layout and Design Philosophy

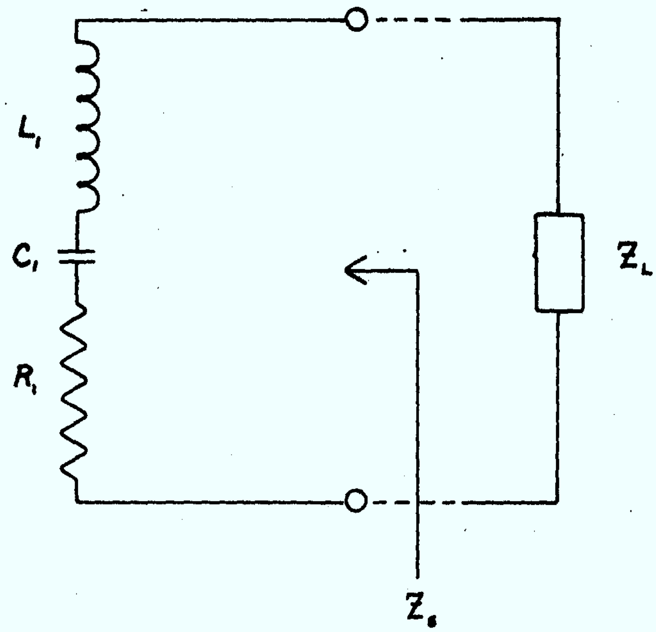

Figure 3.7a: Series Equivalent Circuit of an Oscillator

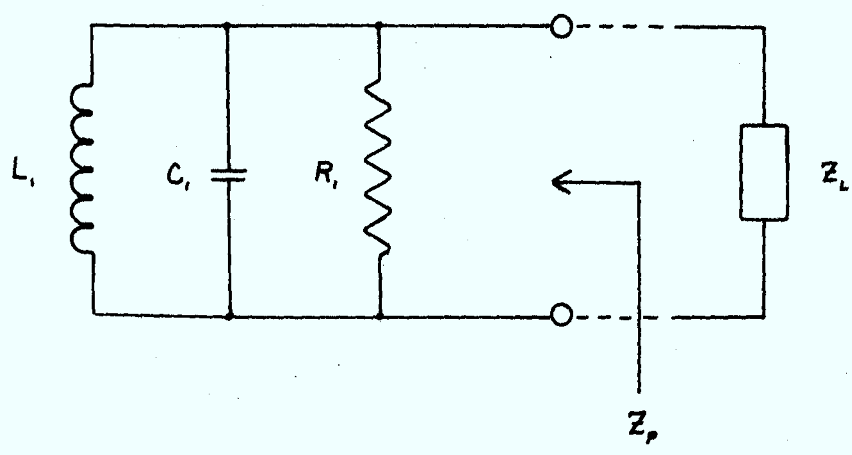

Figure 3.7b: Parallel Equivalent Circuit of an Oscillator

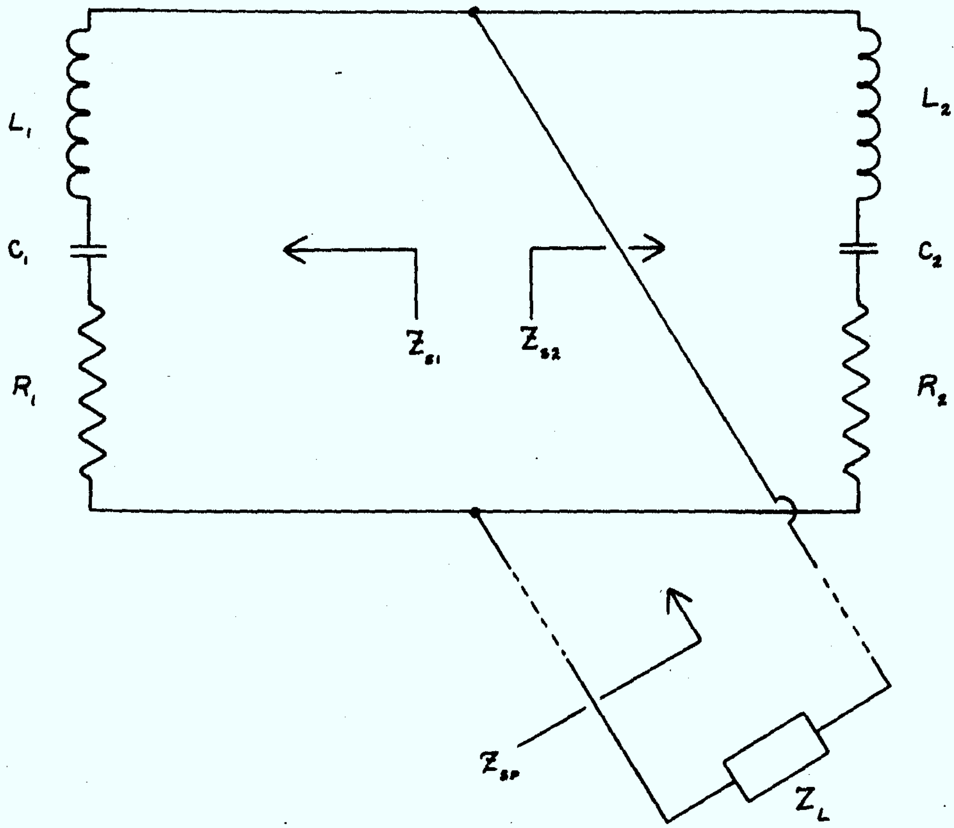

Figure 3.8a: Parallel Combination of Two Series Equivalent Circuits

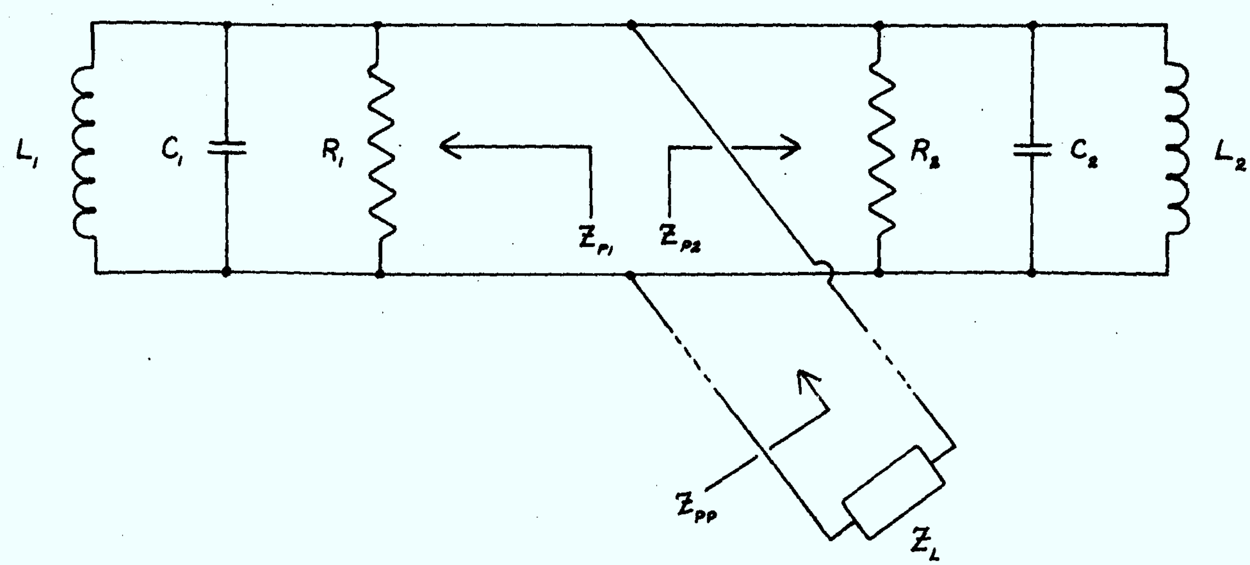

Figure 3.8b: Parallel Combination of Two Parallel Equivalent Circuits

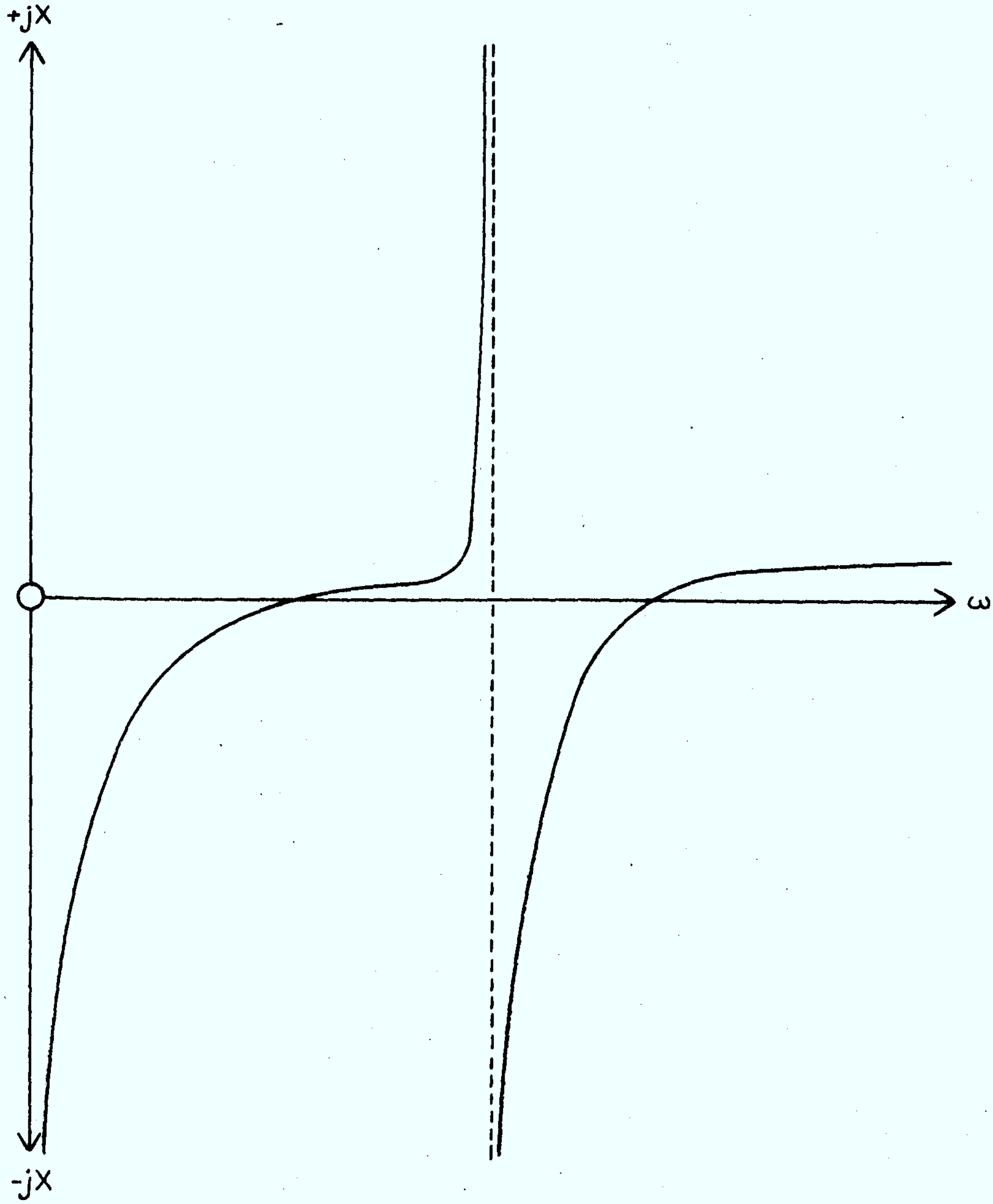

Figure 3.9 Graphical Representation of the Function $Z_{sp}(\omega)$

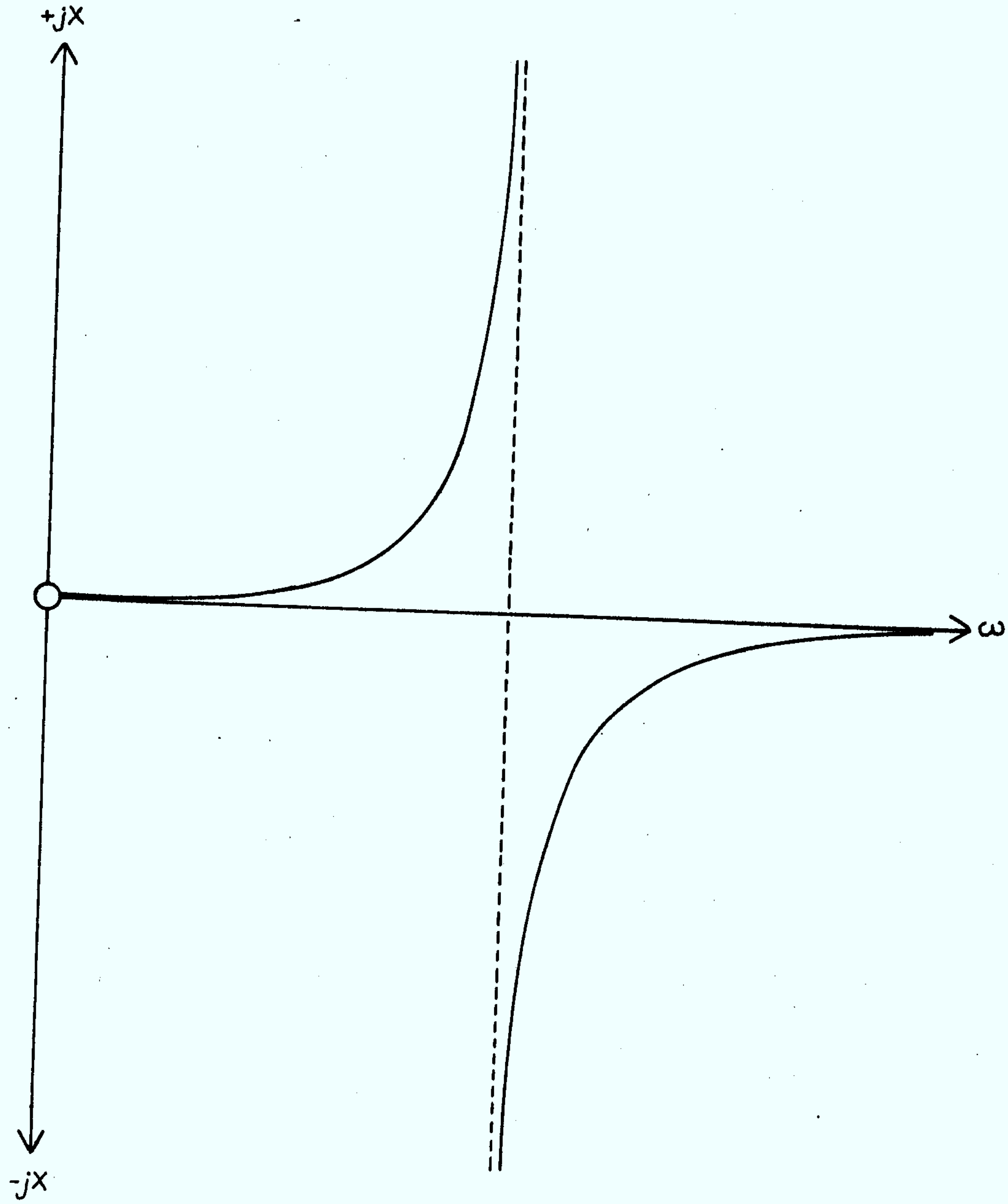

Figure 3.10 Graphical Representation of the Function $Z_{pp}(\omega)$

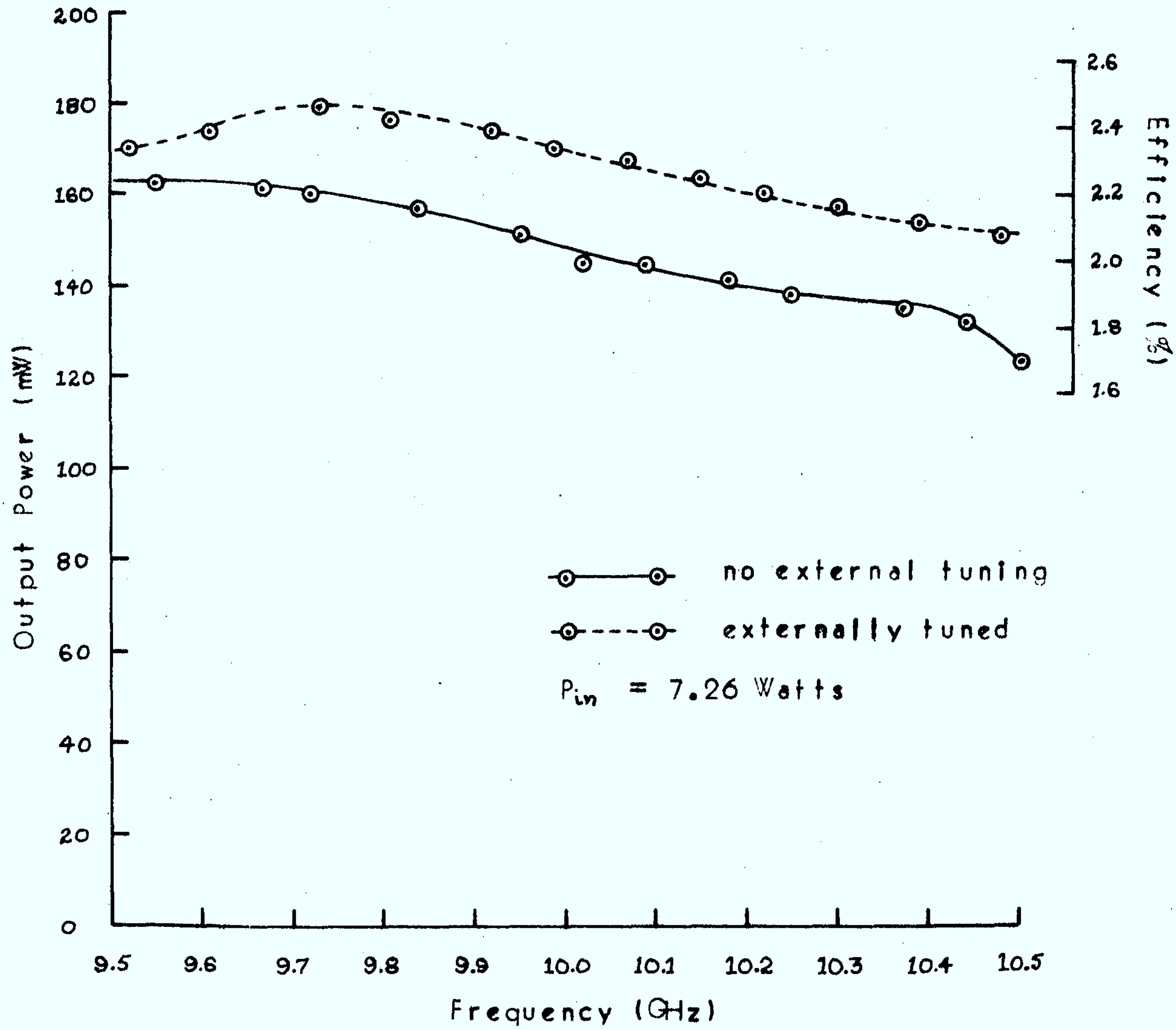

Figure 3.11; Output Power and Efficiency vs Frequency for Circuit Configuration B4

(Results corrected for testbed losses - see Appendix C)

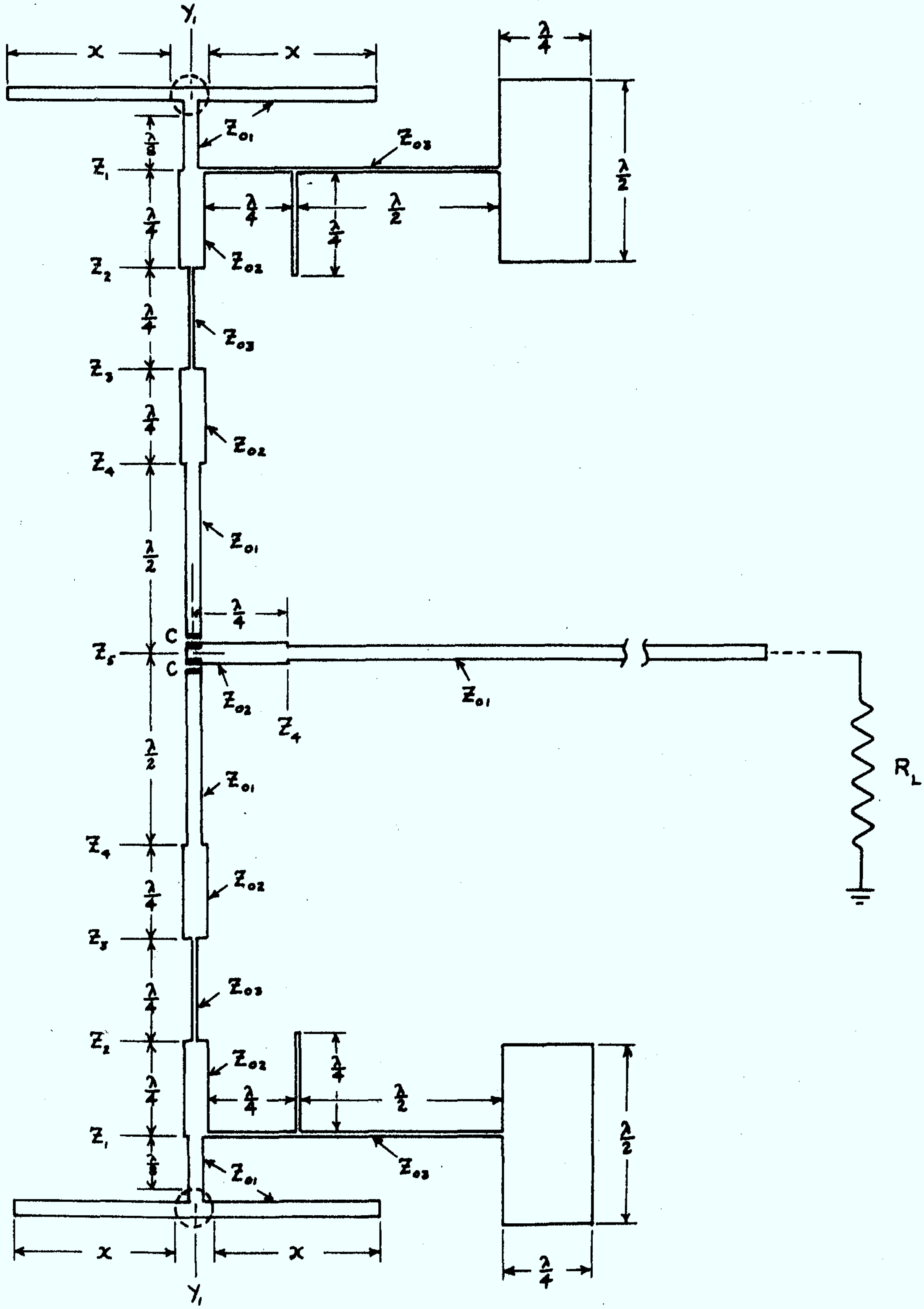

Z_{01} = 50 ohms	Z_1 = 2.5 ohms	Y_1 = 2-j20 millimhos
Z_{02} = 35 ohms	Z_2 = 490 ohms	R_L = 50 ohms
Z_{03} = 104 ohms	Z_3 = 22 ohms	C = 100 pf
	Z_4 = 50 ohms	x - variable
	Z_5 = 25 ohms	

Figure 3.12 Circuit Layout and Design Immittance Values for Circuit Configuration B5

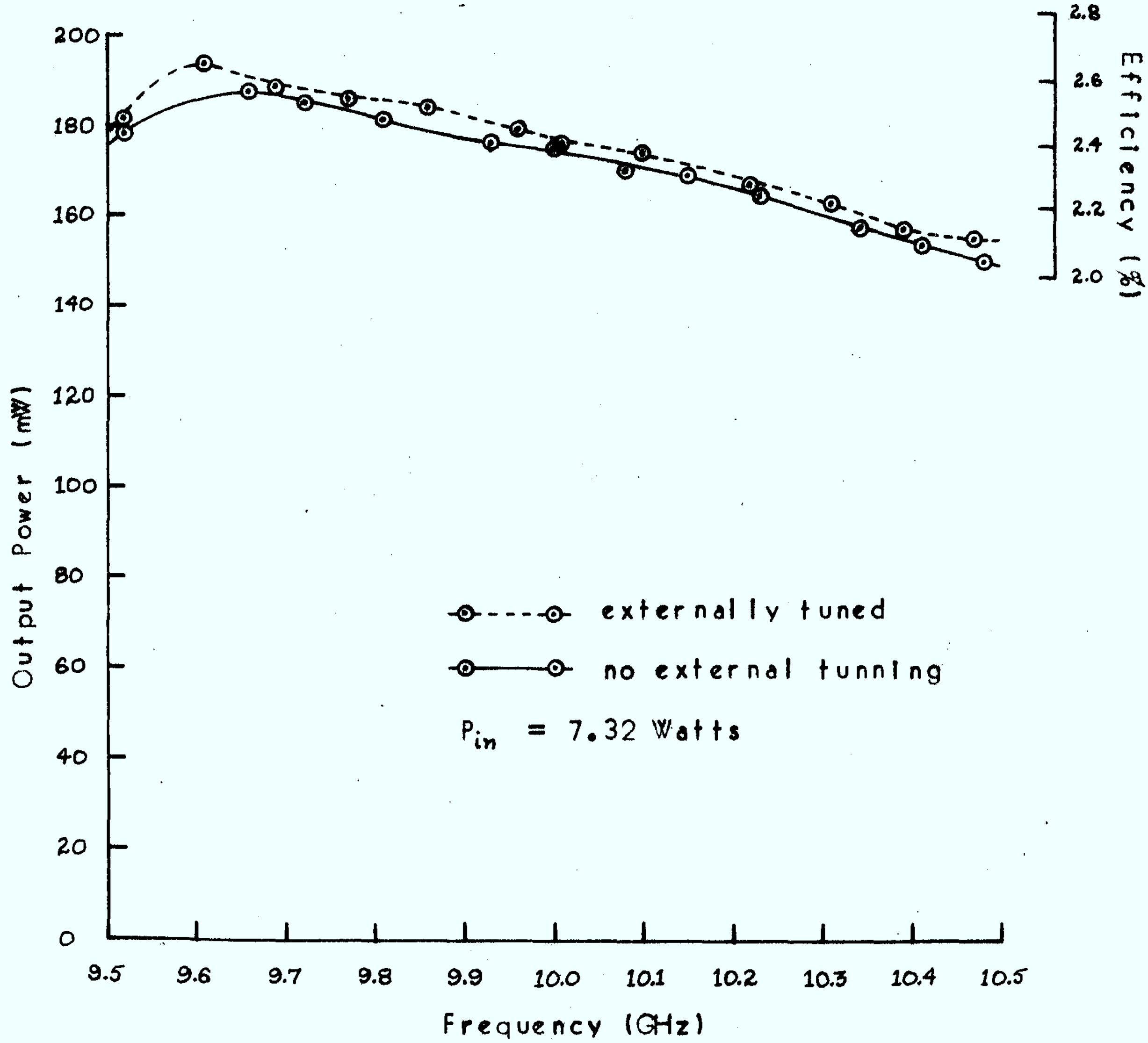

Figure 3.13: Output Power and Efficiency vs Frequency for Circuit Configuration B5

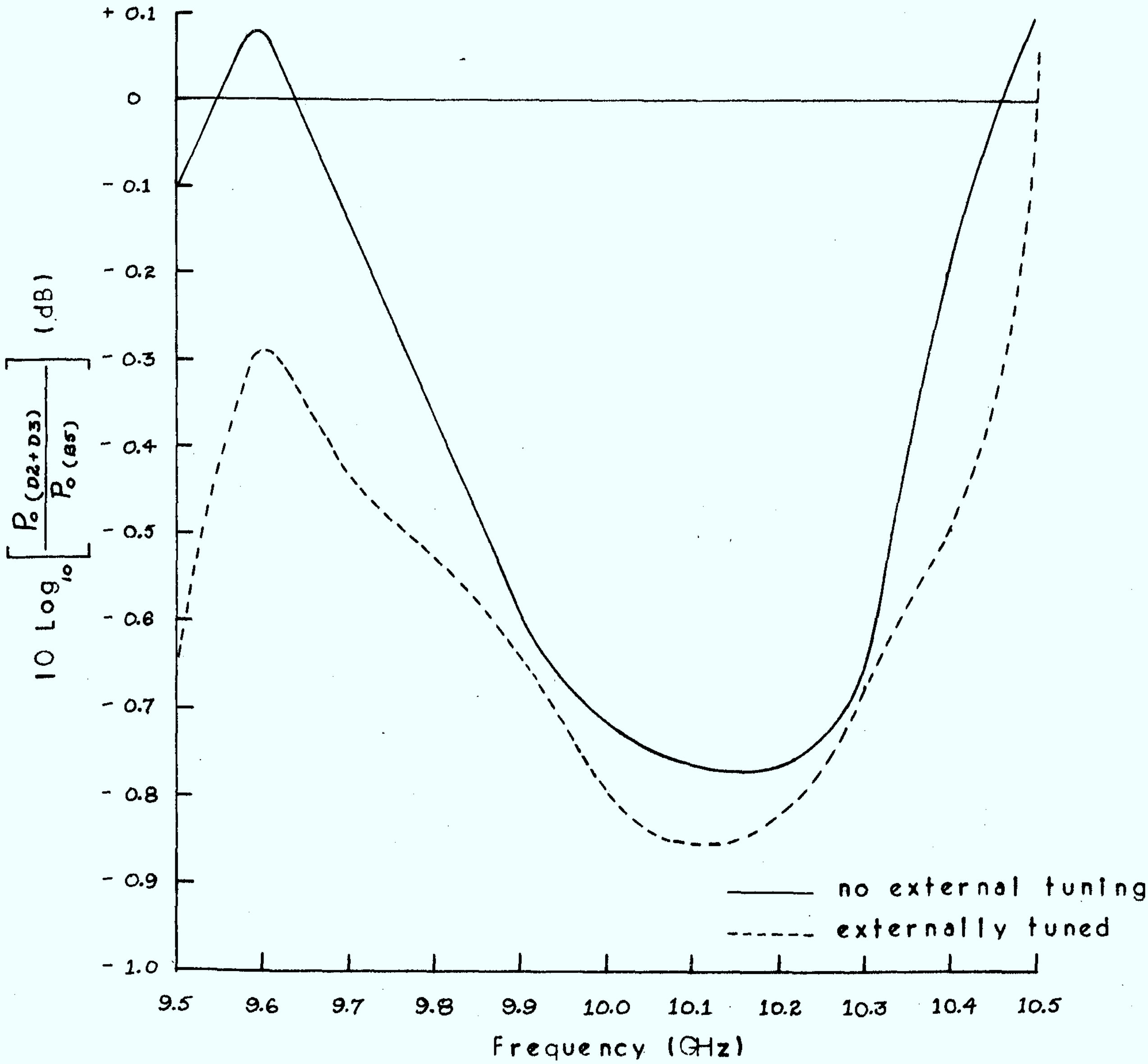

Figure 3.14: Comparison Between the Output Power from Diodes D2 and D3 Operating in Single-Device Circuits and the Output from Circuit Configuration B5.

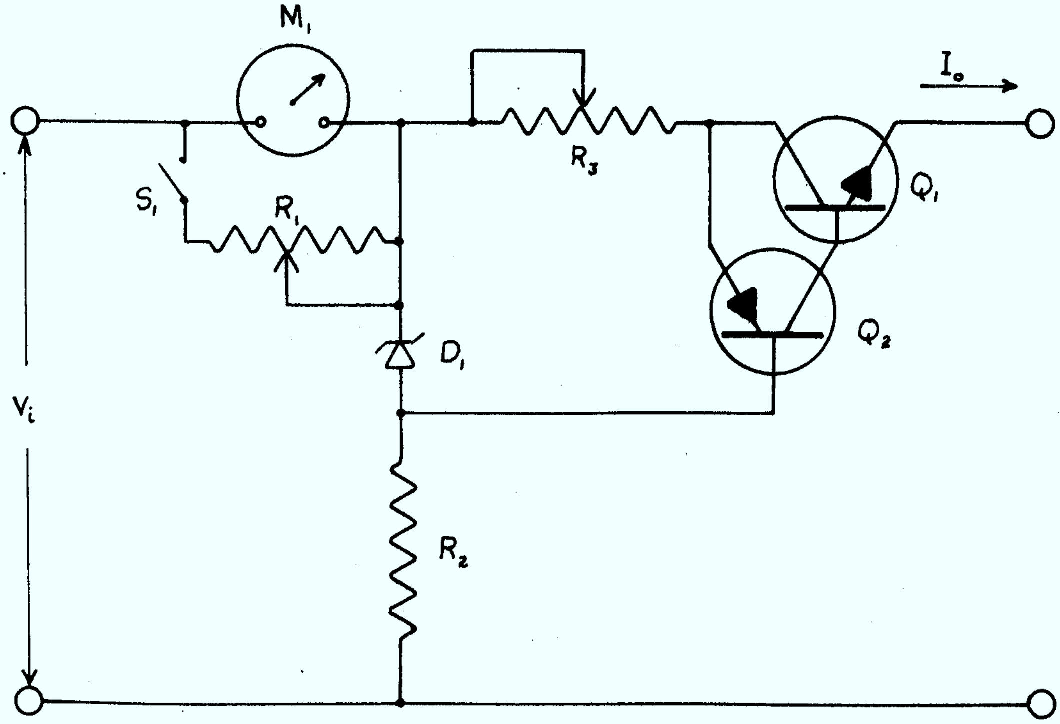

M_1 - milliammeter, 0-50 mA
S_1 - milliammeter x2 range switch
R_1 - 500 ohms, meter calibration (x2 range)
R_2 - 100 K ohms
R_3 - 250 ohms, current control
D_1 - 1N4733, 5.1 Volt zener
Q_1 - 2N3440
Q_2 - 2N5416
V_i - 100 VDC
I_o - constant current output

Figure B1: Constant Current Regulator Circuit

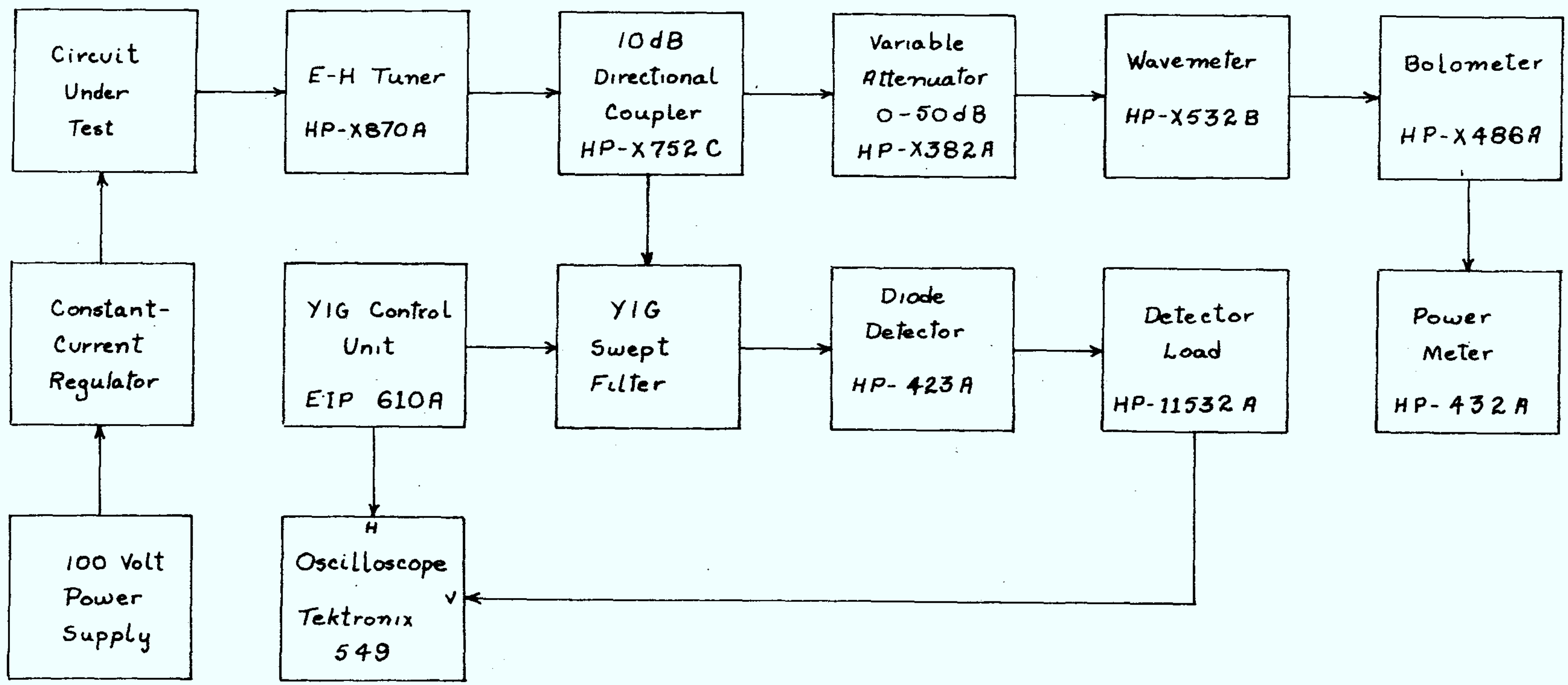

Figure C1: Block Diagram of the Testbed

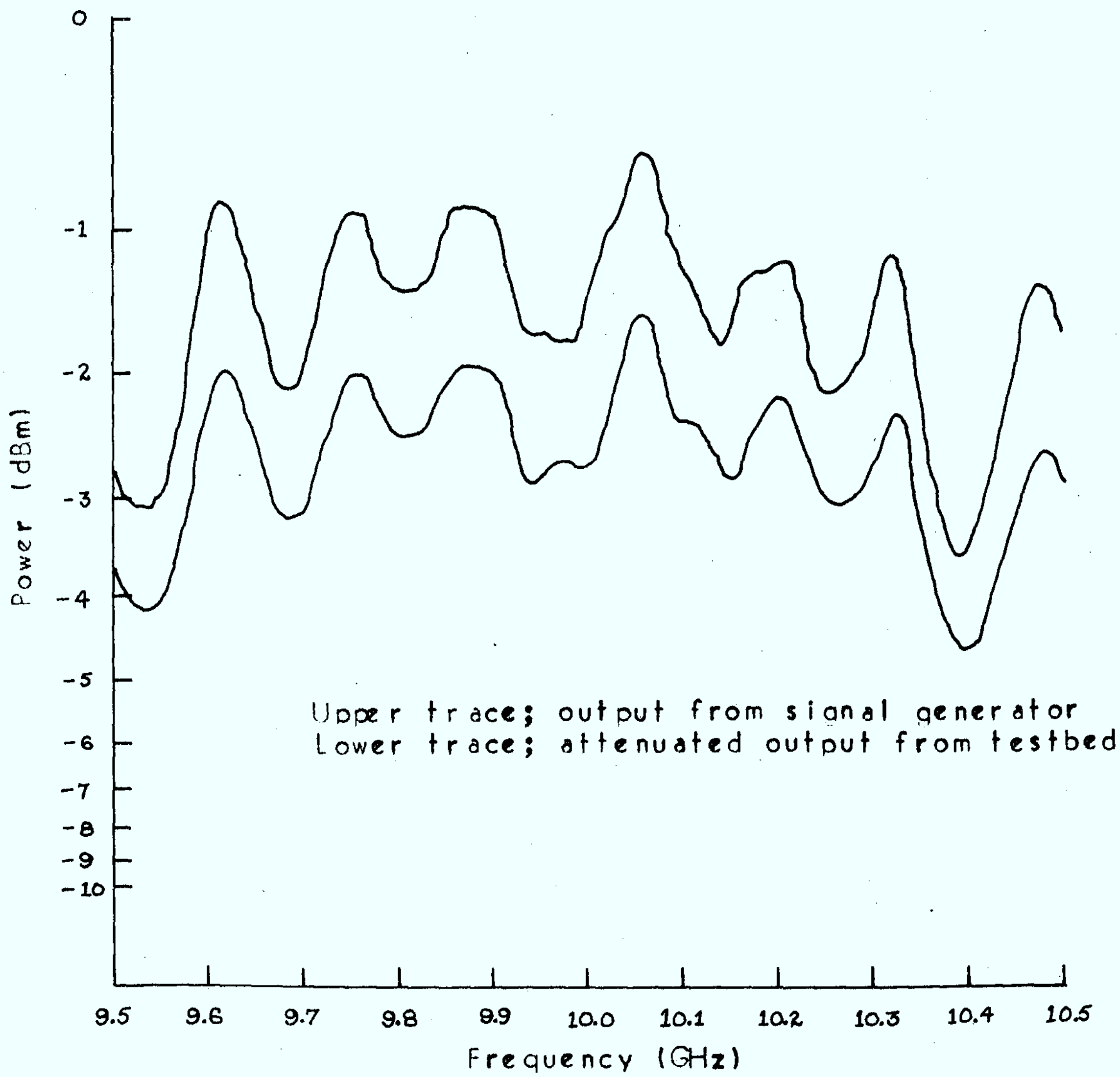

Figure C2: Testbed Attenuation as a Function of Frequency

BIBLIOGRAPHY

1. F.A. Brand, "System Potential of Microwave Solid State Generation and Amplification", Proc. 3rd Biennial Cornell Electrical Engineering Conference, p. 26, August 1971.

2. C.B. Swan, T. Misawa and L. Marinaccio, "Composite Avalanche Diode Structures for Increased Power Capability", IEEE Trans., Electron Devices, Vol. ED-14, No. 9, pp 584-589, September 1967.

3. A.M. Cowley, and R.C. Patterson, "High-Power Parallel-Array IMPATT Diodes", Electronics Letters, Vol. 7, No. 11, pp 301-303, 3 June 1971.

4. S. Mitsui, "CW Gunn Diodes in Composite Structure", IEEE Trans., Microwave Theory and Techniques, Vol. MTT-17, No. 12, pp 1158-1160, December 1969.

5. J.E. Carroll, "Series Operation of Gunn Diodes for High R.F. Power", Electronics Letters, Vol. 3, No. 10, pp 455-456, October 1967.

6. F.M. Magalhaes and W.O. Schlosser, "A Series Connection of IMPATT Diodes", Proc. IEEE, Vol. 56, No. 5, pp 865-866, May 1968.

7. P.K. Blair, A. Pearson, and S. Heeks, "250 Watt Module Using Series Operated Gunn Diodes", Proc. 3rd Biennial Cornell Electrical Engineering Conference, pp 309-313, August 1971.

8. S. Boronski, "Parallel-Fed CW Gunn Oscillators Cascaded in X-Band Waveguide for Higher Microwave Power", Electronics Letters, Vol. 4, No. 10, pp 185-186, 17th May 1968.

9. W.O. Schlosser, and A.L. Stillwell, "A Travelling-Wave Approach to the High-Power Solid-State Oscillator", Proc. IEEE, Vol. 56, No. 9, p. 1588, September 1968.

10. F. Ivanek, and V.G.K. Reddi, "Modular Approach to Higher-Power Avalanche-Diode Oscillators", Electronics Letters, Vol. 4, No. 21, 18th October 1968.

BIBLIOGRAPHY (Cont'd)

11. C.T. Rucker, "A Multiple-Diode High-Average-Power Avalanche-Diode Oscillator", IEEE Trans., Microwave Theory and Techniques, Vol. MTT-17, No. 12, pp 1156-1158, December 1969.

12. K. Kurokawa, "An Analysis of Rucker's Multidevice Symmetrical Oscillator", IEEE Trans., Microwave Theory and Techniques, Vol. MTT-13, No. 11, pp 967-969, November 1970.

13. D.F. Kostishack, "UHF Avalanche Diode Oscillator Providing 400 Watts Peak Power and 75 Percent Efficiency", Proc. IEEE, Vol. 58, pp 1282-1283, August 1970.

14. R.J. Chaffin, and E.P. EerNisse, "A Poor Man's TRAPATT Oscillator", Proc. IEEE, Vol. 58, pp 173-174, January 1970.

15. R.J. Socci, and R.I. Harrison, "A Multidiode Avalanche Oscillator for Increased C.W. Microwave Power Output", Proc. IEEE, Vol. 54, pp 1006-1007, July 1966.

16. H. Fukui, "Frequency Locking and Modulation of Microwave Silicon Avalanche Diode Oscillators", Proc. IEEE, Vol. 54, pp 1475-1477, October 1966.

17. G. Luzzatto, "An N-Way Hybrid Combiner", Proc. IEEE, Vol. 55, pp 470-471, March 1967.

18. S. Mizushina, "2 Oscillators Combined with 3-dB Directional Couplers for Output Power Summing", Proc. IEEE, Vol. 55, pp 2166-2167, December 1967.

19. H.J. Kuno, J.F. Reynolds, and B.E. Berson, "Push-Pull Operation of Transferred-Electron Oscillators", Electronics Letters, Vol.5, No. 9, pp 178-179, 1st May, 1969.

20. K. Kurokawa, and F.M. Magalhaes, "An X-Band 10-Watt Multiple-IMPATT Oscillator", Proc. IEEE, Vol. 59, pp 102-103, January 1971.

21. K. Kurokawa, "The Single-Cavity Multiple-Device Oscillator", IEEE Trans., Microwave Theory and Techniques, Vol. MTT-19, No. 10, October 1971.

BIBLIOGRAPHY (Cont'd)

22. F. Assadourian, and E. Rimai, "Simplified Theory of Microstrip Transmission Systems", Proc. IRE, Vol. 40, pp 1651-1657, December 1952.

23. M. Caulton, J.J. Hughes, and H. Sobol, "Measurements of Microstrip Transmission Lines for Microwave Integrated Circuits", RCA Review, Vol. 27, pp 377-391, September 1966.

24. R.A. Pucel, D.J. Masse, and C.P. Hartwig, "Losses in Microstrip", IEEE Trans. Microwave Theory and Techniques, Vol. MTT-16, No. 6, pp 342-350, June 1968.

25. L. Lewin, "Radiation from Discontinuities in Strip Line", Proc. IEE, Vol. 107, Pt.C, pp 163-170, February 1960.

26. O.P. Jain, "A Study of Dispersive Behavior in Microstrip Transmission Lines", Carleton University, Faculty of Engineering Technical Report, May 1971.

27. O.P. Jain, V. Makios, and W.J. Chudobiak, "Open-End and Edge Effect in Microstrip Transmission Lines", IEEE Trans. on Microwave Theory and Techniques, Vol. MTT-20, No. 9, pp 626-628, September 1972.

28. The Microwave Engineer's Handbook and Buyer's Guide, Horizon House - Microwave, Inc., Dedham, Massachusetts, pp 65-66, 1969.

29. W.J. Chudobiak, private communication, May 1972.

30. E.C. Jordan, and K.G. Balmain, "Electromagnetic Waves and Radiating Systems", Prentice-Hall, Inc., New Jersey, 2nd ed., 1968, p 219.

31. ibid, pp 230-231.

32. J. Reed, and G.J. Wheeler, "A Method of Analysis of Symmetrical Four-Port Networks", IRE Trans., Microwave Theory and Techniques, Vol. MTT-4, No. 10, pp 246-252, October 1956.

BIBLIOGRAPHY (Cont'd)

33. G.R. Harrison, G.H. Robinson, B.R. Savage, and D.R. Taft, "Ferrimagnetic Parts for Microwave Integrated Circuits", IEEE Trans., Microwave Theory and Techniques, Vol. MTT-19, No. 7 pp 577-588, July 1971.

34. E.C. Jordan, and K.G. Balmain, "Electromagnetic Waves and Radiating Systems", Prentice-Hall, Inc., New Jersey, 2nd ed., 1968, p 227.

35. G.V. Welch, and T.K. Ishii, "Hybrid-Tee Coupled Oscillators", Electronics Letters, Vol. 6, No. 22, pp 712-718, 29th October 1970.

36. "Microwave Power Generation and Amplification Using IMPATT Diodes", Hewlett-Packard Application Note 935, Hewlett-Packard, Palo Alto, California, pp 8-9.